

NCC2-912 Ames Research Center  
Seti Institute  
Report in Place of Performance Rpt.

NASA-CR-201461

LMMS-P421026  
January 31 1996

1-10  
7-1-96  
0.95  
61170

---

---

## PHYSICAL CHARACTERIZATION OF SiO<sub>2</sub> AEROGEL

### PHASE II FINAL REPORT

Subcontract Number: 565-9204

---

---

Submitted to:

**SETI Institute**  
2035 Landings Drive  
Procurement Operations  
Mountain View, CA 94043

Prepared by:

**J.T. Ryder, J.P. Wittenauer, D.J. Mendez**

LOCKHEED MARTIN



Lockheed Martin Missiles & Space  
Advanced Technology Center  
3251 Hanover Street  
Palo Alto, California 94304

## ACKNOWLEDGMENTS

We are indebted to the many contributors to this report. The most notable ones are listed; if we have left someone out, our sincere apologies.

### **LMMS, Advanced Technology Center**

At the LMMS ATC, we thank:

- o Mr. Joseph F. Cullinan (Organization 93-60) for his dedication to produce finished ACCs for deployment on the Mir;
- o Mr. Robert N. Hall, Jr. (Organization 93-50) for his microphotography of many difficult subjects;
- o Mr. Allen H. Heynen (Organization 93-60) for his detailed SEM and EDS analytical work in determining the morphological and elemental characteristics of hypervelocity particles and the corresponding aerogel capture media;
- o Mr. Les Fisher (Organization 93-60) for his sustained efforts in running the Hypercritical Solvent Extraction System to produce aerogel and to prepare the aerogel for use in ACCs;
- o Mr. James G. Moncur (Organization 93-50) for his perseverance and dedication in development of mass spectrometer techniques for trace level organic analysis of aerogels and for his track and particle organic amino acid analysis.

### **LMMS, Sunnyvale**

At LMMS in Sunnyvale, we thank:

- o Ms. Eva Buchan (Organization 81-12) for her CTH modeling and analysis used for hypervelocity particle impacts on aerogel;
- o Mr. Erik R. Matheson (Organization 81-12) for his preliminary finite analysis to be used for particle impact analysis on variable density aerogels.

### **SETI Institute, NASA ARC, and Universities**

In addition we also wish to acknowledge:

- o Dr. Ted Bunch, Project Scientist, NASA ARC, for his valuable technical suggestions and supply of the cometary materials;
- o Mr. Kenji Nishioka, SETI Institute, for his keen technical contributions, report review, and overall guidance;
- o Mr. Wayne Logsdon, and the other CALSPAN HVGR support personnel, whose able direction, help, patience and long hours of support during the test launches made this report possible and also for their significant, even primary, contributions to the development of the sabot concept used in this study;
- o Dr. Peter Schultz, Chairperson of the Hypervelocity Vertical Gun Range National Facility, Professor Geology, Brown University, for his valuable suggestions and assistance with the HVGR operation.

## GLOSSARY OF TERMS &amp; ABBREVIATIONS

amu	Atomic Mass Unit
ARC	Ames Research Center
ACC	Aerogel Capture Cell
AELD	Analysis Event Logic Diagram
BET	Brunauer, Emmett, and Teller (Inventors of the method for measuring nitrogen gas sorption on material using a volumetric method).
BLINT	Boundary Layer Algorithm for Sliding Interfaces
C	Unit of Temperature, Centigrade
cc	Unit of volume, Cubic Centimeters
CDP	Cosmic Dust Particle
CDSP	Cosmic Dust Simulant Particle
CEP	Circular Error Probability
CJ	Chapman-Jouguet
CJVB	Chapman-Jouguet Volume Burn (an option in the CTH model)
CTH	In 1969 a major report on hydro code was published by Sandia. The report was titled "CHARTD" which stood for "Coupled Hydrodynamics and Radiation Transport Diffusion." This work was extended and the result was called "CSQ" which stood for "CHARTD Squared" which really represents adding the second dimension, not the process of squaring. Then came the 80s when the addition of another computational dimension, i.e., CTH, or "CHARTD-to-the-Three Halves Power" was created; thus, CTH stands for "Coupled Hydrodynamics and Radiation Transport Diffusion Performed in One, Two, or Three Dimensions."
DH/GC/MS	Dynamic Headspace, Gas Chromatography, Mass Spectrometer
DNP	Dinitrophenyl
EDS	Energy Dispersive Spectrometer
EOS	Equation of State
FEM	Finite Element Analysis
FT-IR	Fourier Transform - Infrared
g	Unit of mass, gram
GC/MS	Gas Chromatography Mass Spectrometer
HVG	Hypervelocity Vertical Gun
HVGR	Hypervelocity Vertical Gun Range
IDP	Interplanetary Dust Particle
K	Unit of temperature, Kelvin
km	Unit of distance, Kilometer
LMSC	Lockheed Missiles and Space Company, Inc.
L-N <sub>2</sub>	Liquid Nitrogen
LS	Launch Series
MDL	Minimum Detection Limit
mg	Unit of mass, Milligram
mm	Unit of length, millimeter
NASA	National Aeronautics and Space Administration
NDE	Non-destructive Evaluation
Pa	Unit of pressure, Pascal
PAH	Polycyclic Aromatic Hydrocarbon
ppb	Parts per Billion
ppm	Parts per Million
psi	Unit of pressure: Pounds per square inch
sec	Unit of time, Second
SEM	Scanning Electron Microscope
SETI	Search for Extra-Terrestrial Intelligence Institute
SiO <sub>2</sub>	Silicon Dioxide
SPM	Scanning Probe Microscope
WDS	Wavelength Dispersive Spectrometer

## FOREWORD

This Phase II Final Report was prepared by the Lockheed Martin Missiles and Space (LMMS) Advanced Technology Center and is submitted to the SETI Institute in fulfillment of Phase II Subcontract Number 565-9204. This report summarizes (1) the results of tests conducted to measure artificially induced entrained contamination and improvements in CTH modeling, (2) contamination sources in the sol-gel and aerogel processes; (3) aerogel fabrication and storage contamination issues; (4) aerogel instrument integration including general handling, machining and contamination processes; (5) procedures which minimize contamination during storage of aerogel and during preflight conditions, and (6) procedures for handling aerogel during flight boost, orbit and reentry phases. Included in the Final Report are the procedures used to design, fabricate, and test aerogel capture cells (ACC) as flight modules for a SETI/NASA ARC/University of Paris collaborative cosmic dust capture experiment on Mir. Included are the results of vibration tests on an ACC module. The lessons learned from producing actual flight hardware are discussed.

## CONTENTS

<b>Section</b>	<b>Title</b>	<b>Page</b>
	ACKNOWLEDGMENTS	i
	GLOSSARY OF TERMS & ABBREVIATIONS	ii
	FOREWORD	iii
<b>1.0</b>	<b>INTRODUCTION AND EXECUTIVE SUMMARY</b>	<b>1-1</b>
1.1	BACKGROUND	1-1
1.2	APPROACH	1-2
1.3	PURPOSE, GOALS, AND OBJECTIVES	1-2
1.4	SUMMARY OF RESULTS	1-3
1.4.1	PROGRAM ACHIEVEMENTS	1-3
1.4.2	KEY PROBLEMS ENCOUNTERED	1-4
1.4.3	RECOMMENDED FOLLOW-ON RESEARCH	1-5
<b>2.0</b>	<b>AEROGEL PURITY AND ORGANIC CONTAMINATION SOURCES</b>	<b>2-1</b>
2.1	CHEMICAL ANALYSIS METHODS	2-1
2.1.1	DYNAMIC HEADSPACE GC/MS ANALYSIS FOR EVALUATING AEROGEL PURITY	2-4
2.1.2	SOLVENT EXTRACTION AND DERIVATIZATION GC/MS ANALYSIS FOR GLYCINE	2-5
2.2	AEROGEL PURITY AND SOURCES OF CONTAMINATION	2-5
2.3	AEROGEL CAPTURE MEDIA PURITY	2-8
2.3.1	AEROGEL PROCESSING IMPURITIES	2-8
2.3.2	AEROGEL PURITY	2-8
2.4	AEROGEL OPTICAL TRANSMISSIVITY	2-16
2.4.1	TRANSMISSIVITY MEASUREMENT AND DATA ANALYSIS	2-16
2.4.2	FACTORS EXPECTED TO INFLUENCE OPTICAL TRANSMISSIVITY	2-16
2.4.3	OBSERVATIONS REGARDING LMSC AEROGEL TRANSMISSIVITY	2-17
<b>3.0</b>	<b>CONTAMINATION ENTRAINMENT</b>	<b>3-1</b>
3.1	EXPERIMENTAL CONDITIONS	3-1
3.2	EXPERIMENTAL RESULTS	3-1
3.2.1	ORGANIC ENTRAINMENT	3-1
3.2.2	CONTAMINATION DIFFUSION	3-4
3.2.3	POST LAUNCH ORGANIC DIFFUSION INTO AEROGEL	3-5
3.2.4	AEROGEL SURFACE DEBRIS REMOVAL	3-5
3.3	CONCLUSIONS	3-5
<b>4.0</b>	<b>CTH MODELING OF THE IMPACT PROCESS</b>	<b>4-1</b>
4.1	INITIAL MODELING CONDITIONS	4-1
4.2	CTH MODELED AEROGEL TRACKS	4-4
4.3	OTHER PROFILES	4-7
4.4	CONCLUSIONS	4-8
<b>5.0</b>	<b>APPLICATION TO PRACTICE: DESIGN, FABRICATION, AND LAUNCH OF AN AEROGEL FLIGHT MODULE</b>	<b>5-1</b>
5.1	AEROGEL CAPTURE CELL REQUIREMENTS	5-1
5.2	AEROGEL CAPTURE CELL DESIGN	5-1
5.2.1	HARDWARE DESIGN	5-1
5.2.2	AEROGEL SPECIFICATION	5-2
5.2.3	ASSEMBLY METHODOLOGY	5-2
5.3	AEROGEL CAPTURE CELL FABRICATION	5-2

<b>Section</b>	<b>Title</b>	<b>Page</b>
5.3.1	ACC HARDWARE FABRICATION	5-2
5.3.2	AEROGEL SYNTHESIS	5-3
5.3.3	BONDING PROCEDURES	5-5
5.4	AEROGEL CAPTURE CELL TESTING AND EVALUATION	5-9
5.4.1	OUTGASSING ANALYSIS	5-9
5.4.2	SHOCK AND VIBRATION ANALYSIS	5-9
5.5	PROCEDURES FOR SHIPMENT AND STORAGE	5-10
5.6	SUMMARY	5-11

## LIST OF ILLUSTRATIONS

<b>Figure</b>	<b>Title</b>	<b>Page</b>
2.3-1	CHROMATOGRAPH OF LM CLEAN "HIGH-PURITY" AEROGEL	2-9
2.3-2A	CHROMATOGRAPH OF EXAMPLE LM "HIGH-PURITY" AEROGEL	2-12
2.3-2B	CHROMATOGRAPH OF EXAMPLE LM CLEAN "HIGH-PURITY" AEROGEL	2-12
2.3-4	CHROMATOGRAPH OF "COMMERCIAL" AEROGEL	2-15
2.4.3-1	OPTICAL TRANSMISSIVITY DATA FOR ACC-QUALITY AEROGEL	2-18
2.4.3-2	RAYLIEGH SCATTERING PARAMETER ANALYSIS	2-18
3.2.1-1	PICTURE AND DIAGRAM OF TRACK FOR LS4-8	3-2
3.2.1-2	VOLUME ELEMENT ALONG TRACK OF LS4-8 USED FOR GLYCINE ANALYSIS	3-3
3.2.1-3	PLOT OF GLYCINE ANALYSIS RESULTS FOR TRACK OF LS4-8	3-4
4.1-1	PHOTOGRAPH OF A 6.7 JOULE PARTICLE TRACK IN AEROGEL	4-4
4.1-2	TRACK DIAGRAM	4-5
4.1-3	CARNELIAN PARTICLE CAPTURE IN AEROGEL	4-5
4.2-1	AEROGEL PLOT: 0.0 SEC	4-6
4.2-2	AEROGEL PLOT: 10.0 $\mu$ SEC	4-6
4.2-3	AEROGEL PLOT: 30.0 $\mu$ SEC	4-6
4.2-4	AEROGEL PLOT: 55.0 $\mu$ SEC	4-6
4.3-1	POSITION HISTORY	4-7
4.3-2	VELOCITY HISTORY	4-7
4.3-3	KINETIC ENERGY HISTORY	4-7
4.3-4	PARTICLE THERMAL PROFILE	4-7
4.3-5	EXPANDED VIEW OF THE PARTICLE AT 55 $\mu$ SECONDS	4-9
4.3-6	DENSITY CONTOUR PLOT AT 55 $\mu$ SECONDS	4-9
4.3-7	AEROGEL TEMPERATURE CONTOUR PLOT AT 55 $\mu$ SECONDS	4-10
5.2.1-1	SCHEMATIC OF AEROGEL CAPTURE CELL	5-2
5.3.2-1	AEROGEL TILE WITH ONE FACE SHEET REMOVED FROM MOLD	5-3
5.3.3.1	LIQUID METAL ENCAPSULATION PROCEDURE	5-5
5.3.3-2	AS-BONDED ACC UNIT	5-6
5.3.3-3	FINAL ACC ASSEMBLY SHOWING ACC UNIT AND LID	5-7
5.3.3-4	THREE-RAIL PLATEN USED TO COMPRESSIVELY LOAD AEROGEL TILE	5-8
5.3.3-5	FAMILY OF SEVEN ACCs PRIOR TO PACKAGING FOR SHIPMENT	5-8

**LIST OF TABLES**

<b>Table</b>	<b>Title</b>	<b>Page</b>
1.3-1	GOALS AND OBJECTIVES	1-3
2.1-1	GC/MS ANALYSIS METHODS	2-2
2.2-1	MANUFACTURE AND INSTRUMENT ASSEMBLY OF AEROGEL ACCs	2-6
2.2-2	FACTORS THAT AFFECT AEROGEL PURITY	2-7
2.3-1	EXAMPLE OF PURITY LEVELS OF LM "HIGH-PURITY" AND LM CLEAN "HIGH-PURITY" AEROGEL	2-11
2.3-2	EXAMPLE OF PURITY LEVELS OF LM "NOMINAL" AND LM CLEAN "NOMINAL" AEROGEL	2-13
2.3-3	RESIDUAL IMPURITIES FOUND IN "COMMERCIAL" AEROGEL	2-14
2.3-4	QUALITATIVE COMPARISON OF THE LM CLEAN HIGH-PURITY AEROGEL TO OTHER AEROGELS AND TO FOAMS	2-15
3.2.1-1	GLYCINE ANALYSIS RESULTS FOR TRACK OF LS4-8	3-3
4.1-1	PARTICLE TRACER LOCATIONS	4-2
4.1-2	EXPERIMENTALLY DETERMINED IMPACT PARAMETERS OF LS4-8	4-3
5.3.2-1	CHEMICAL ANALYSIS OF EXTRACTED AND BAKED AEROGEL	5-4
5.3.3-1	CHEMICAL ANALYSIS OF AEROGEL WITNESS COUPON	5-6
5.4.2-1	SHOCK AND VIBRATION TESTING	5-9

## SECTION 1.0

### INTRODUCTION AND EXECUTIVE SUMMARY

The objective of this research was to develop procedures that, when followed, will assure that the process for capturing Interplanetary Dust Particles and debris preserves as much data of impacting particles in aerogel as possible. The procedures were developed to minimize inadvertent internal and external contamination throughout all phases of capture media development and pre- and post-flight analysis of the aerogel capture media. Procedures were reviewed to minimize sample contamination problems that might be introduced due to the analysis operations themselves which would be performed on the capture media. The individual physical, chemical, and testing procedures for each step of the various processes were defined. In the future, the procedures must be tested and executed with significant care and with a documented archive of each starting and ending point. This will provide clear traceability of any test to confirm the accuracy of the test results obtained on real cosmic organic, hydrocarbon, or other trace compounds captured in the aerogel media based on needs described by the exobiology research community. As an application of the above practices, an aerogel module was designed and several modules were manufactured for use in a joint NASA ARC/SETI/University of Paris flight experiment to be flown on the Russian Mir space station. These modules were filled with aerogel, sealed, and delivered to SETI for incorporation with the University of Paris EuroMir experiment modules. They are being flown on the Mir beginning in October 1995 and into about March 1996.

This report documents the results of the Phase II experimentation and analysis associated with the capture of dust particle simulants, traveling with kinetic energies equivalent to those expected for actual particles, using full size aerogel capture modules. The report also contains a summary of the experience of building actual flight modules containing aerogel. The report has several purposes.

- o Present the procedures used to obtain high purity aerogel and the associated result of using those procedures.
- o Discuss the contamination sources for all phases of aerogel processing through orbital deployment to Earth return and post processing of any captured particles.
- o Measure the survivability and entrainment of contamination which may be on the surface of the capture module at the time of particle impact into IDP tracks.
- o Evaluate the migration of surface contamination over a 6 month period after the surface has been contaminated with a known concentration of contaminant.
- o Update the CTH model developed for aerogel/particle penetrations in Phase I using the high penetration characteristics measured for several particles.
- o Identify and evaluate the problems with aerogel instrumentation and associated aerogel handling to minimize contamination. This includes:
  - Aerogel Bulk handling and capture cell development;
  - Pre-flight, flight, and post-flight procedures; and
  - Post-flight particle extraction and particle handling.
- o Design and construct Aerogel Capture Cells for the NASA ARC/SETI/University of Paris particle capture experiments to be flown on the Russian Mir space station.

#### 1.1 BACKGROUND

Particles orbiting the Sun and Earth have material compositions ranging from man-made debris to interplanetary dust particles (IDPs) including cosmic dust. This research is motivated by the desire to address several issues of interest about the nature of these materials. The first area of interest concerns obtaining information on the chemical and physical processes that occurred during



condensation of the solar nebula and subsequent accretion of matter into planetary bodies. A traceability path consisting of biogenic elements, their relative distribution, and the formation processes leading to simple compounds and complex molecules may be derivable from interplanetary particles thereby shedding light on the origin of life. A second area of interest is the potential identification and characterization of interstellar grains which may be components of dust particles that predate the solar system, or of contemporary grains from IDPs including comets and primitive meteorites that are intercepted while they cross the inner solar system. Finally, a third area of interest is a better understanding of the nature of the man-made particles found in low-Earth orbit and of the collision hazards they pose to spacecraft.

To address these issues, dust particles should ideally be captured in a way that both preserves the physical characteristics of the particles and maintains their physical size. In this research work the capture media being studied is aerogel. Since the particles of interest are quite small, typically less than 15 microns, the ability to provide a means of selective identification of each particle, their extraction from the aerogel capture media, and their subsequent analysis is difficult. Certain issues that have an obvious impact on the use of aerogels as a capture media have not been evaluated in this research. These issues include the influence of solar radiation on aerogels, static charge buildup on the surface and interior of the aerogels while the aerogels are exposed in orbit, general contaminating dust collected on the surface of the aerogel, and thermal cycling of the aerogel under the conditions of having embedded instrumentation, or not, and the influence of the transport environment (vibration specifically) for both orbital insertion and recovery after incurring multiple impacts.

## **1.2 APPROACH**

The Hypervelocity Vertical Gun Range (HVGR) located at NASA Ames Research Center was used to accelerate IDP simulants to kinetic energies in the range of the upper limit of those found in space. The simulant particles were impacted into aerogel. An analysis was performed which typifies the bounds of contamination which can be expected during aerogel fabrication, use, and archival storage. The basic aerogel handling procedures and the steps necessary to quantitatively document chemical integrity are put forth. The physical and chemical properties of aerogel were investigated as was the potential of organics on the aerogel surface to diffuse into and contaminate the aerogel volume over time. A primary task in this research was to determine how well organics entrained on the particles survive and are preserved by the capture process, and whether contaminating organics on the aerogel surface and entrained by the impacting particles can be measured thus determining whether the original particle organics can be identified. Thus, the particles and resultant penetration tracks were analyzed for survival of entrained organic materials originally on the particles, and for contamination by organic materials originally on the surface of the aerogel. The basic approach was to provide controlled aerogel samples, hypervelocity particles, a controlled "contamination" compound, and a controlled environment allowing inference of the capture media performance. An experiment was conducted to determine if an aerogel capture module surface can be cleaned once it is recovered from space. All of these experiments were conducted to reduce the probability that the measurement of native organics on or in a particle would be masked by contamination from manufacturing, handling, and space-born contamination caused by man-made environmental effects of the type found in the near-space of the deployed platforms. Finally, aerogel capture cells were designed, fabricated, delivered for use on the NASA ARC/SETI/University of Paris particle capture experiment which is to be deployed on the Russian Mir.

## **1.3 PURPOSE, GOALS, AND OBJECTIVES**

The purpose and goals of this research are given in Table 1.3-1.

<b>Table 1.3-1: Goals and Objectives</b>			
<b>Purpose</b>	<b>Goal</b>	<b>Achievement Status</b>	<b>Report Section</b>
1. Summarize aerogel manufacturing and chemical analysis procedures	Present chemical analysis data showing that high purity aerogel was manufactured	High purity aerogel was manufactured	2
2. Evaluate aerogel contamination sources	Develop a table of potential sources of aerogel contamination	Sources were identified and tabulated	2
3. Evaluate Effect of Surface Contamination	Measure Entrainment of Surface Organics	Some organics are entrained and survive the capture process	3
4. Measure Organic Diffusion in Aerogel	Quantify Diffusion Characteristics	For the selected control organics, no diffusion problems identified	3
5. Find ways to clean ACC Surface Adsorbed Contamination	Eliminate space borne contamination on ACC	A potentially effective means for eliminating ACC surface debris was demonstrated	3
6. CTH Modeling	Further evaluate CTH model applicability	Track characteristics well modeled, but physically unreal assumptions were required raising issues of general applicability	4
7. Identify Shipping and Storage Problems	Develop procedure to minimize contamination risk in the storage process	Procedure developed, tested, and found to be valid	5
8. Identify ACC orbital handling procedures	Develop practical recommendations for handling ACCs in boost, orbit, deployment, recovery, and reentry phases	Procedure developed based on HVGR testing procedures and practices	5
9. Evaluate practicality of procedures	Design, fabricate, and test ACC for use on Russian Mir	ACCs were designed, fabricated, successfully tested and deployed on Mir	5

## 1.4 SUMMARY OF RESULTS

### 1.4.1 Program Achievements

This report is the second and final report on a program to investigate the use of aerogel as an IDP capture media. The previous Phase I Final Report had several conclusions listed in Section 1.0 of that report. To those conclusions, an additional list is given below based on the results reported in this Phase II Final Report.

- Dynamic Headspace GC/MS was shown to be a reliable chemical analysis procedure to evaluate aerogel product purity.
- Solvent Extraction and Derivatization GC/MS was shown to be a reliable chemical analysis procedure to detect aliphatic amino acids, such as Glycine, within aerogel.
- Techniques were defined to produce high purity aerogel.

- The primary factors which affect aerogel purity were identified.
- Aerogel was manufactured which had less than 1 ppm of any impurity other than residual methanol.
- The purity of the manufactured aerogel product was much better than commercially available aerogels and of foams proposed as IDP capture media.
- The transmissivity of the aerogel product was shown to be excellent with an associated scattering coefficient of  $C = 0.0160 \mu\text{m}^4\text{cm}^{-1}$ , a value indicative of a good level of transmissivity.
- The factors expected to influence optical transmissivity were identified and some of them evaluated.
- An organic “contaminant” on the surface of the aerogel can be entrained with an IDP track during the impact event.
- An organic “contaminant” on the surface of the aerogel does not tend to diffuse into the aerogel volume after a 180 storage time.
- An organic “contaminant” within an IDP track in the aerogel does not tend to diffuse into the surrounding aerogel volume.
- A laser beam method was found to be successful in removing embedded carbon on the surface of the aerogel. Electron beams and neutral plasmas were not successful in removing the surface carbon.
- The CTH model evaluated as a method to model tracks in aerogel produced by impacting IDPs when updated with new empirically based parameters was found to model the aerogel track fairly well. However, the model resulted in an unrealistic and physically impossible compression of the particle plus required unrealistically high yield strength and spall stress which perhaps implies potentially significant shortcomings in this modeling approach.
- Aerogel Capture Cells were successfully designed, manufactured, integrated into space flight hardware and deployed on the Russian MIR space station. The aerogel attachment scheme was validated and shock and vibration tests successful completed.

#### 1.4.2 Key Problems Encountered

The following is a summary of the key problems encountered and the status of their resolution.

##### 1. Problem: Test Environment

**Issue A:** The HVGR has a pressure wave of hydrogen which arrives with significant force to severely compress the aerogel. The wave also contains carbon “contaminant” particles. Although the modifications to the HVGR described in the Phase I Final Report alleviated much of the problem, the issue remains for future use of the HVGR.

**Issue B:** Modification to the sabot used in the HVGR, as described in the Phase I Final Report, proved to be highly successful, however the level and type of contamination which may occur on the surface of the aerogel due to that on the sabot remains an unresolved issue.

##### 2. Problem: Aerogel Purity

**Issue A:** The relative importance of all of the factors which influence aerogel has not yet been determined. While high purity aerogels were consistently produced, the level of manufacturing care required is not yet fully identified.

**Issue B:** Chemical analysis techniques to detect the full range of potential organic materials which could potentially be found in the aerogel after capture of an IDP are not yet available.

**Issue C:** The relative importance of the factors which influence aerogel transmissivity has not yet been determined.

### **3. Problem: Aerogel Cracking**

**Issue:** During manufacture of the aerogel, cracking would often occur within the aerogel. Although many aerogel blocks were produced essentially crack free, many were not. Future work is required to further understand the cause of the cracking. At present, cracking is known to be related to the surface finish of the mold and to the processing cycle.

### **4. Problem: Modeling of IDP Impact Event**

**Issue:** Although the CTH model selected to model IDP impact into aerogel, when modified, gave predictions of track shape and depth similar to those actually observed, several physically unrealistic assumptions had to be made to achieve such agreement. Alternatives to such assumptions have not yet been identified.

### **5. Problem: Manufacture of Aerogel Capture Cells**

**Issue:** The as-baked aerogel apparently has extreme reactivity. This reactivity manifested itself in two ways.

- On the initial bonding trial, the glass platen used to counter the buoyancy forces associated with the liquid metal encapsulation became physically bonded to the aerogel tile. A solution was to construct a platen from three quartz tubes. Using these tubes as rails, a compressive load could be applied to the aerogel with the minimum possible surface blemishing.
- The aerogel absorbed MEK and acetone that were stored in squeeze bottles in a far corner of the exhaust hood where the liquid metal encapsulation was taking place. The aerogel must be protected from exposure to such organic solvents in future efforts.

#### **1.4.3 Recommended Follow-On Research**

Based on the results of this study, recommendations for follow-on research are summarized below.

- Analyze and evaluate the engineering performance of recovered ACCs flown on Mir in collaboration with University of Paris' Comrade experiment.
- Develop, plan and conduct the necessary research to resolve the problems encountered in maintaining the purity of the cleaned aerogel while being integrated into the capture cell for the Comrade experiment.
- Assemble a systematic procedure for locating and recovering micron to 10's of micron particles embedded in an ACC.
- Design, fabricate, and test a breadboard integrated ACC instrument composed of trajectory and time of impact sensor, aerogel capture cell, and electronics to capture and store necessary data.
- Develop techniques to identify other amino acids and organics that may be found in aerogel after capture of IDPs.
- Define the details of a chemical analysis protocol for ACCs containing IDPs.
- Further evaluate the effect of a particle impacting into surface "contaminated" aerogel on the extent of entrained organic within the aerogel track.

- Compare the results of the CTH model of particle impact tracks with that obtained using other modeling approaches.
- Investigate several research questions related to aerogel transmissivity. They include investigating the effects on optical transmissivity of: impurities; moisture; aerogel spatial uniformity; manufacturing processing variables, such as gelling time, and extraction procedures; aerogel cell and particle size, and; long term aging.
- Related to optical transmissivity, other issues should be investigated for aerogel being subjected to long term aging, such as (a) does the aerogel become more cloudy with time, (b) can the cloudiness be reversed (by bake cleaning, for example), and (c) the cause of cloudiness, if it occurs (exposure to light, absorption of moisture, etc.).

## SECTION 2.0

### AEROGEL PURITY AND ORGANIC CONTAMINATION SOURCES

Because a primary reason to capture IDPs is to detect organic materials, the purity of the aerogel material is of prime importance as is the maintenance of that purity when particles are captured. Aerogel visual clarity also is a key issue for the location and identification of particles and particle tracks as a part of an overall investigative plan to capture and analyze IDPs. Optical transmissivity (clarity) itself may serve as a valuable qualitative assessment tool for indicating aerogel density, uniformity, and cleanliness. In this section, chemical and transmissivity analyses methods and results are discussed. The analyses methods were used to (a) evaluate the purity of the aerogel product, (b) detect a representative amino acid, glycine, (c) evaluate aerogel transmissivity, and (d) evaluate the factors that affect aerogel purity and transmissivity. Comparisons of aerogel product purity to other materials also are discussed. Due to funding constraints, many of the results are preliminary.

#### 2.1 CHEMICAL ANALYSIS METHODS

Chemical analysis methods were selected to evaluate the purity of the aerogel product and to detect glycine. A chemical analyses method for evaluating the purity of the manufactured aerogel was selected after considering a wide range of Gas Chromatography Mass Spectrometry (GC/MS) methods, other types of mass spectrometry, gas chromatography without mass spectrometry, and such methods as laser spot analysis. A method also was selected to detect glycine, which was used as a representative amino acid and introduced into the aerogel in specific experiments as described in the Phase I Final Report and in Section 3 of this report. Method selection was based on a problem solution approach within the cost and schedule constraints of the program. The selected methods proved to be more than adequate for the program needs. No attempt was made to select and define rigorous chemical analysis methods for use in detecting organic molecules that might be introduced into the aerogel by IDPs. Detection of organic molecules introduced by IDPs would have required the selection and development of many complimentary analysis methods and procedures. This was beyond the scope of this investigation.

For this study, primarily low molecular weight (MW) organics were of interest ( $< \sim 300$  amu) because the solvents employed in aerogel manufacture, the byproducts of the sol-gel and aerogel formation processes, and the amino acid glycine all have relatively low MWs (generally below 300 amu). In general, solvents tend to have molecular weights below 100 amu, liquids have MWs up to about 300, and solids MWs above 300. There are, of course, some unusual liquids or solids that have lower or higher MWs. There also are molecules, such as water ( $\text{H}_2\text{O}$ ) and methanol ( $\text{CH}_3\text{OH}$ ) that have a low molecular weight but act and are detected as if they are high molecular weight molecules because of strong molecule to molecule interactions due to their hydrogen bonds.

Gas Chromatography Mass Spectrometry (GC/MS) was selected as the primary analysis method both to assess aerogel product quality and to detect the presence of glycine. Aerogel is particularly amenable to GC/MS analysis because the open porous structure allows extraction of volatile and semi-volatile organics by either thermal or solvent means. The drawback to the GC/MS method is that molecules of molecular weight less than 40 amu are not well captured by the L-N<sub>2</sub> cryotrap used in the method. Carbon dioxide ( $\text{CO}_2$ , MW 44 amu) is the lowest weight molecule usually detected by GC/MS. Thus selection of the GC/MS method eliminated detection of both fairly stable molecules [such as methane ( $\text{CH}_4$ ), ammonia ( $\text{NH}_3$ ), ethylene ( $\text{C}_2\text{H}_4$ ), ethane ( $\text{C}_2\text{H}_6$ ), carbon monoxide ( $\text{CO}$ ), oxygen ( $\text{O}_2$ ), and nitrogen ( $\text{N}_2$ )] and unstable molecules [such as acetylene ( $\text{C}_2\text{H}_2$ )]. Detection of such very low molecular weight molecules was not considered critical to this study because the molecular weights of the aerogel impurities and the amino acid glycine that needed to be detected were expected to be above 40 amu. Detection of very low weight molecular molecules may be of critical scientific interest, however, their detection would require either different or additional analysis techniques, or both.

Many sensitive analysis methods are available using GC/MS. Four well known methods useful for detection of the low molecular weight organics that were expected to be found in the aerogel product are listed in Table 2.1-1. The thermal extraction method known as Dynamic Headspace GC/MS (DH/GC/MS) was selected to assess the purity of the manufactured aerogel product. This was because the compounds of interest primarily were either residual solvents or non-polar, low molecular weight organics produced during aerogel manufacture. Both of these classes of organics would have been obscured if aerogel purity had been analyzed by solvent extraction. Although the Solvent Extraction GC/MS was very useful for detecting glycine, the method was not used to quantify aerogel purity. The method causes a major portion of the early chromatogram to be overwhelmed with the solvent used and the numerous impurities. In addition, the impurities of solvents are usually similar molecules as those expected to be found in the aerogel product. Even if partially useful, the solvent extraction method, by itself, does not give significantly lower minimum detection limits than Dynamic Headspace GC/MS. This is because when solids are extracted in solvents the extract can only be concentrated by a modest amount, due to solvent impurities, and only a small amount of the solvent extract can be injected into a GC column (e.g. 2-5 microliters of a typical 100 microliter concentrated solvent extract). Additional chemical information on aerogel purity could possibly have been gained using the Direct Probe/MS method. However, the Direct Probe method is not as accurate as the DH/GC/MS for detecting the expected impurities in the aerogel left by manufacture.

Table 2.1-1 GC/MS Analysis Methods

GC/MS Method	Description	Comments
1. Dynamic Headspace	Thermal desorption in helium (conducted at 200°C, could go up to 300°C) with cryotrapping at -196°C followed by GC/MS of outgasses	Good for analyzing aerogel product purity; Not good for detecting amino acids; Many molecules significantly fractionate above 200°C
2. Solvent Extraction and Derivatization	Uses silylating agents (like 1:1 mixture of acetonitrile with [BSTFA 99%/TMCS 1%, Alltech #18087]) to make non-volatile, ionic, thermally labile amino acids into volatile organics that can pass through a GC column without degradation	Good for analyzing amino acids; Not good for analyzing aerogel product purity; An extension of the traditional solvent extraction method
3. Solvent extraction	Traditional method of extraction	Not good for analyzing aerogel product purity because solvent obliterates much of the data; Not good for detecting amino acids without derivatization; Many molecules significantly fractionate above 200°C
4. Direct Probe/MS	Small sample heated in ion source region (vacuum)	Not good for analyzing aerogel product purity; Not good for detecting amino acids; Many molecules can significantly fractionate

The Solvent Extraction and Derivatization GC/MS method of Table 2.1-1 was selected to detect glycine. The DH/GC/MS method was not used because amino acids primarily exist as polar, ionic, low molecular weight organics which are not easily detected by DH/GC/MS. For the same reason, DH/GC/MS also is not particularly suitable to detect peptides. The Solvent Extraction method was not used by itself because the ionic amino acid would not be clearly detected without a derivatizing agent. The Direct Probe method was not used because the method can not detect amino acids. In the Solvent Extraction and Derivatization GC/MS method, the solvent extract can be concentrated, giving added sensitivity, and can be readily quantified. Thus the method is a very good analysis technique for detecting amino acids, such as glycine, and peptides where the solvent and its impurities does not obscure detection of the amino acid. However, the solvent still must be very pure because the initial purity limits the resultant sensitivity obtained by extract concentration. For ionic amino acids, such as glycine, the chosen solvent also must be a silylating, derivatizing agent to convert the ionic amino acid into a covalent thermally stable molecule for chromatography analysis. Because only a small amount of the solvent extract can be injected into a capillary column, (e.g. 2 microliters), potentially the method's sensitivity can be much less than that of the DH/GC/MS method (which could not be used, as previously mentioned). Still, the method proved to be quite useful for detecting the glycine used in the experiments of this study.

Both DH/GC/MS analysis for aerogel product purity and Solvent Extraction and Derivatization GC/MS analysis for glycine were conducted using a Fisons 70SEQ Mass Spectrometer. This instrument, when operated at a medium to low mass resolution of 1,000 ( $m_1/m_1-m_2$ ), can readily detect 10 picograms of most low molecular weight organics. This is significantly better resolution and sensitivity than that obtained with quadrupole mass spectrometers which can generally only detect 10 picograms of selected organics in full scan mode, despite claims to the contrary in the commercial literature. Some mass spectrometer manufacturers misleadingly cite sensitivity based on an arbitrary compound, such as hexachloro benzene, which has a very favorable ionization behavior and fragmentation pattern. The Fisons double focusing, magnetic sector mass spectrometer gives more reproducible sensitivity than quadrupole mass spectrometers because it uses high voltage ion acceleration which is much less sensitive to ion source contamination build-up.

Other analyses methods are possible using GC/MS, mass spectrometers of other types, or using gas chromatographs without mass spectrometry. Pyrolysis GC/MS, for example, while allowing investigation of materials that might be bound to the aerogel, was not used because the high temperature during pyrolysis fragments organics. This could result in misinterpretation of the original nature of the impurities that were within the aerogel after its manufacture. The method may be of scientific value for analyzing aerogels which contain IDPs because at least the presence of organics from IDPs might be inferred based on the detection of fractured organics. However, the precise nature of the original organics generally could not be ascertained using pyrolysis GC/MS. Analysis of organics using a GC without mass spectrometry also was not conducted because of the method's inability to reliably identify unknown molecules. Although Ion Trap Mass Spectrometry can detect organics, this method was not used because only aromatic stabilized organic molecules exhibit molecular ions. Potentially, this method could not identify many of the organics of interest in this study, such as aliphatic compounds, which lack the critically important molecular ions. Again, the method may be of scientific value for analyzing aerogels used to capture IDPs.

Laser spot analysis would be a quick alternate method to detect organics, especially stable solids, that may be introduced into the aerogel by IDPs. However, to date, we have seen no evidence that amino acids can be detected using this method. Since, in this study, the amino acid glycine was analyzed for its presence after being deliberately introduced into aerogel products, laser spot analysis was not used. There is evidence that PAHs could be detected by laser spot analysis. Thus the method might be useful for investigating aerogel containing IDPs provided that one accepts the potential of not detecting amino acids that may actually be present and accepts that the method tends to fragment organics resulting in the same interpretation issues as for the pyrolysis GC/MS method.



### 2.1.1 Dynamic Headspace GC/MS Analysis for Evaluating Aerogel Purity

The analysis procedure for the Dynamic Headspace GC/MS method is described in detail in the Phase I Final Report, Appendix B. The approach is based on a widely cited method by Moncur, et al<sup>1</sup> for thermal extraction. Dynamic Headspace GC/MS analysis uses thermal desorption in a helium flow cell with cryotrapping (at -196°C) followed by GC/MS analyses of outgasses. The helium flow cell allows the choice of thermal desorption conditions, typically 200°C to 300°C for 15 minutes to 1 hour. The desorption products are present in the helium carrier gas as it moves from the sample flow cell into the column. This helium flow is split, typically set to discard 97% with 3% going into the column. The minimum detection limits cited below include consideration of a typical 33:1 splitting away of the carrier gas. The flow going into the column is later detected in the ion source which ionizes the gasses, using a spiraling electron beam, and accelerates them, using a large potential field. Higher temperature desorption conditions are helpful in desorbing higher molecular weight, higher boiling point organics, but they tend to cause more artifacts in the apparatus due to the outgassing of non-metal parts. In addition, temperatures above 200°C result in fragmentation of many organics, which are generally thermally labile up to 200°C. The molecular weight range of organics typically detected using a 200°C desorption temperature is from 10 to 500 gram/mole, (up to 1000-1500 gram/mole for polydimethyl siloxanes). A 260°C desorption temperature, the highest practical temperature, readily detects organics up to 600 g/mole, and even higher molecular weight siloxanes, but with fragmentation of other organics.

When using the Dynamic Headspace GC/MS method for analysis of aerogel purity, standards at known concentrations were analyzed to establish the experimentally derived sensitivity. For future work, organic standards should be analyzed frequently to fully document instrument sensitivity, minimum detection limit, accuracy, and precision of the instrument. A blank was run each day after the apparatus was first baked to document the identity and quantity of artifacts present, such as CO<sub>2</sub> from room air that gets into the cell when the sample is loaded. Typically, a 10 mg sample was wrapped in a 4 mil thick aluminum foil "cigarette." The foil was pre-cleaned with a heat gun at 500°C in air and previously desorbed and tested in the blank run. Organic molecules that are desorbed from aerogel at the chosen conditions were trapped at liquid nitrogen temperature (-196°C) as the flexible fused silica GC capillary column was immersed in liquid nitrogen during the sample desorption step. The actual GC/MS analysis was comprised of a high resolution GC separation (distillation) and electron impact mass spectrometric analysis of the GC column outlet gas. The mass spectrometer was scanned over a mass range of choice, typically every one second for 45 minutes.

The Fisons 70SEQ mass spectrometer can detect low molecular weight organics with various minimum detection limits using the Dynamic Headspace GC/MS mode. As the purity of the manufactured aerogel increased during the program, the minimum detection limits were decreased by adjusting the instrument and experimental procedures.

1. In the **Normal sensitivity work**, conducted early in this study, 5-10 mg samples of aerogel were used and typically 0.3 nanograms ( $0.3 \times 10^{-9}$  gm) of low molecular weight organics were detectable by the mass spectrometer. This gave a minimum detection limit (MDL) in the range of 1-3 parts-per-million (ppm, v/v concentration) when operating the mass spectrometer at medium sensitivity, (typical, medium detector voltages at 50%).
2. For the **Higher sensitivity work**, conducted later in the study, again using 5-10 mg sample sizes, the system easily detected 10 picograms ( $1 \times 10^{-11}$  grams) of most low molecular weight organics (MW<300 g/mole) that eluted from the column into the ion source when set up for medium high sensitivity. These conditions gave an MDL in the range of 0.01-0.03 ppm (v/v concentration), 10-30 ppb, when operating the mass

---

<sup>1</sup> Moncur, Byrd, Sharp, HRC&CC, Vol. 4, Dec. 1981, pp. 603-611.

spectrometer at medium high sensitivity, (typical, medium high detector voltages at 70-80%).

3. For the **Highest sensitivity work**, which might be necessary in the future, and if approximately 50 mg samples were used, the sensitivity could be further increased by turning up the detector voltage. This should result in an MDL of approximately 1-3 ppb or better. For such studies, a series of standard runs would have to be made in ever decreasing concentrations and the blanks analyzed to verify that no amount of standard carry-over from a previous standard run at a higher concentration is mistaken for the standard near the detection limit of the instrument.

### 2.1.2 Solvent Extraction and Derivatization GC/MS Analysis for Glycine

One of the most sensitive methods for analysis of amino acids involves converting them to non-polar compounds followed by GC/MS analysis. The analysis procedure for the Solvent Extraction and Derivatization GC/MS method used in this study is described in detail in the Phase I Final Report, Appendix A. In the experiments, derivatization of trace amounts of glycine occurred using the solvent BSTFA (bistrimethyl-silyltrifluoroacetamide) with 1% TMCS (trimethylchlorosilane) in a 1:1 volumetric mixture with acetonitrile ( $\text{CH}_3\text{CN}$ ). The use of silylating agents makes non-volatile, ionic, thermally labile amino acids into volatile organics that can pass through a GC column without degradation. This one step BSTFA/TMCS extraction and derivatization method was used since it has no loss of sensitivity due to clean-up or transfer steps.

The solvent derivatization agent and the detailed procedures were specifically selected to detect the amino acid glycine, which is an aliphatic type amino acid with a molecular weight of about 100 amu. The derivatization agent could be used to detect other aliphatic amino acids, such as Alanine. However, the method would not be good for detecting sulfur based amino acids, such as Cystine, or detecting sterically hindered amino acids. The detection of all amino acids that might be found would require a range of derivatization agents and procedures because they exist in several major forms (aliphatic, hydroxy, sulfur-containing, etc.) and in other less frequently encountered forms. Thus future work to detect amino acids in aerogels containing IDPs will require careful selection and combination of analyses procedures and techniques.

The Fisons 70SEQ gas chromatograph mass spectrometer was again used for glycine detection. In the extraction and derivatization work performed here, the mass of extracted material (i.e. aerogel or IDP simulant) was known as was the instrument response to a known calibrated amount of the amino acid (i.e. glycine). A mass spectrometer response calibration curve was generated over a 10,000 fold or larger glycine concentration range. When the weight of the aerogel (or IDP simulant) was included, a final material concentration MDL could be expressed. This parameter included the current MDL of the instrument (200 femtograms for the most sensitive analyses conducted), plus the weight of extracted material (10 mg), the total BSTFA/TMCS/acetonitrile reagent volume (400  $\mu\text{l}$ ), and the injection volume (2  $\mu\text{l}$ ). Thus the global MDL was approximately 4 ppb ( $4 \times 10^{-9}$  g/g), [global MDL =  $4 \times 10^{-9}$  g glycine/g aerogel (wt/wt),  $5.3 \times 10^{-11}$  mole glycine/g aerogel (mole/wt)].

As an aid to future analysis of aerogel containing IDPs, a fairly large piece of aerogel (e.g. 100 milligram) could be extracted and used to determine the specific amino acids and concentrations found rather than try to analyze a single IDP or track. Other GC/MS techniques, such as Selected Ion Recording (SIR), could potentially be used to obtain instrument MDLs on the order of 1 to 10 femtograms ( $1.3 \times 10^{-17}$  to  $1.3 \times 10^{-16}$  mole) resulting in global MDLs of about 0.2 ppb or less. Such sensitivity was beyond that needed for this study, but might be useful for analyzing aerogels containing IDPs.

## 2.2 AEROGEL PURITY AND SOURCES OF CONTAMINATION

Aerogel was manufactured using a Lockheed Martin developed supercritical extraction system specifically designed to produce high purity aerogel. The manufacture of aerogel and its assembly into a IDP capture instrument involved several steps, as shown in Table 2.2-1: Preparation of Sol-

gel Chemical Precursors, Sol-gel Preparation, Solvent Extraction, Instrument Assembly, and Storage. Not all of the steps were followed for every aerogel that was manufactured. During each step, attention was on the factors that influence aerogel purity and on chemical analysis verification of that purity. In Table 2.2-2 are listed the factors that affect aerogel purity that are amenable to control during aerogel preparation and instrument assembly. Procedures used during Preparation of Sol-gel Chemical Precursors, Sol-gel Preparation, and Solvent Extraction were selected to help assure high purity. During the course of the program, the procedures to manufacture high purity aerogel were modified. Essentially the purity of aerogel product improved throughout the program. As a consequence, the sensitivity of the DH/GC/MS analysis method was increased, as mentioned in Section 2.1. Aerogels produced early in the program were analyzed at an MDL of approximately 1 ppm while those produced later were analyzed at an MDL of approximately 0.01 ppm.

**Table 2.2-1 Manufacture and Instrument Assembly Of Aerogel ACCs**

<b>Manufacture/Assembly Operation</b>	<b>Step</b>
Preparation of Solgel Chemical Precursors	Selection of Chemical precursors Purification Refinement of Chemical precursors (for some cases) Chemical Analysis of Precursor Purity
Sol-gel Preparation	Chemical Mixing Casting in Molds Sol-gel Formation & Curing
Solvent Extraction	Cleaning of HSES Vessel Purity of Process Gases Extraction Process
Instrument Assembly	Removal From Molds Shape Cutting Post Process Cleaning ACC Preparation Integration with ACC Hardware Chemical Analysis of Witness Sample
Storage of Aerogel or Integrated Instruments	Storage Container Design & Construction Placing of ACC into Storage Container Atmospheric Control
Instrument Handling	Pre-Deployment Unpacking of ACC Integration of ACC into Deployment Holder Deployment on Spacecraft Post-Deployment Instrument Handling

**Table 2.2-2 Factors That Affect Aerogel Purity**

<u>Chemical Precursors</u> <ul style="list-style-type: none"> <li>• Water</li> <li>• TMOS</li> <li>• Methanol</li> <li>• Catalyst (Ammonium Hydroxide)</li> </ul>	<u>Solvent Extraction</u> <ul style="list-style-type: none"> <li>• Supercritical Solvent Extraction System</li> <li>• Vessel Cleanliness</li> <li>• Purity of Process Gasses</li> <li>• Process Parameters</li> </ul>
<u>Mixing and Casting</u> <ul style="list-style-type: none"> <li>• Atmospheric Control</li> <li>• Mold Cleanliness</li> <li>• Aging Procedure</li> </ul>	<u>Instrument Assembly</u> <ul style="list-style-type: none"> <li>• Removal from Molds</li> <li>• Cutting to Net Shape</li> <li>• Baking</li> <li>• Integration with ACC Hardware</li> </ul>
	<u>Storage</u> <ul style="list-style-type: none"> <li>• Atmospheric Control</li> </ul>

**Preparation of Sol-gel Chemical Precursors** The precursor sol-gel was formed using distilled water, HPLC grade methanol alcohol, and tetramethoxysilane (TMOS) 99+% pure. Ammonium Hydroxide was used as a catalyst. For “nominal” purity aerogels, chemicals were mixed in a laboratory chemical hood. As an investigation to produce higher purity aerogels, some aerogels were manufactured in a glovebox with a filtered argon gas environment using triply distilled water with the TMOS and methanol initially distilled in the glovebox. In addition, an L-N<sub>2</sub> cold trap was employed in the glovebox to minimize organic contamination. For these aerogels of hopefully higher purity, the catalyst normally used to accelerate the sol-gel formation reaction was not used in an attempt to minimize contamination levels and secondary chemical species which might have been created. Without the catalyst, gelling times often extended to 24 hours or longer.

**Sol-gel Preparation** After mixing, the chemicals were poured into molds which had been pre-cleaned and rinsed several times with the HPLC grade methanol. Pyrex, stainless steel, or aluminum molds were used. Pouring was conducted in a manner that minimized gas bubble formation within the sol-gel. The molds were covered immediately after preparation with clear mylar films to prevent evaporation of the methanol. Sol-gel formation occurred at room temperature while completely submerged in the methanol. For high purity aerogels, sol-gel preparation also was performed in filtered argon gas environment glovebox

Inhomogeneities in the aerogel product were hypothesized to be potentially a cause of cracking within the aerogel during aerogel formation. To help reduce such inhomogeneities and to produce a finer aerogel structure, the chemicals used for some “high purity” aerogels were stabilized at 270°K prior to mixing and pouring into the molds which also had been cooled to 270°K. In such cases, the interior of the molds themselves were pre-coated with a high density SiO<sub>2</sub> sol-gel. This was done based on the hypothesis that such an interior surface would result in less cracking during aerogel formation and in an aerogel with a “better” surface. Once the covered sol-gel formed, the temperature was allowed to return to ambient over a period of three days before putting it into the HSES to produce aerogel.

During the gelling stage of aerogel synthesis, several byproducts are produced. These organics and organosilanes are soluble in methanol, the medium used to age the gel prior to supercritical extraction. By frequently changing to a “fresh” methanol aging bath, during the sol-gel formation process, the concentration of these chemical impurities is made progressively more dilute and the resultant aerogel purity and clarity is expected to improve. However, the cost of the product is increased, since the extra methanol cannot easily be reused and thus must be disposed.

Experiments to date at Lockheed Martin have assessed this factor qualitatively, but it should be assessed quantitatively.

**Solvent Extraction:** The hypercritical solvent extraction system (HSES) was prepared while the sol-gels were forming by filling the unit with methanol of the same grade used to make the sol-gels attaching the argon gas bottles. The molded sol-gels were removed from the glovebox, inserted into the prepared autoclave, immediately covered, and the autoclave extraction process begun. The extraction process of pressurization and heat took place over a period of 1 to 3 days. Extractions were conducted using several different combination of pressure, temperature, and time.

**Post Extraction Cleaning:** To obtain a higher level of purity, some aerogel products were "cleaned" after solvent extraction by using a baking process. The aerogel was placed in a baked-out clean oven and subjected to a flowing high purity oxygen atmosphere at 350°C. In early experiments, these were small samples (e.g. 19 mg) held in stainless steel tubes in flowing O<sub>2</sub> for 1 hr at 350°C. This procedure resulted in improved purity, as shown in Section 2.3. Based on the early successes with this method, the bake cleaning exposure time for aerogels produced later in the program was increased up to 20 hours or more in an attempt to appreciably improve the aerogel purity. Generally, these were larger samples subjected to less direct O<sub>2</sub> exposure.

## 2.3 AEROGEL CAPTURE MEDIA PURITY

The purity of the aerogel product is documented in tabular and graphical formats. Purity levels are compared to a commercially available high purity aerogel and to foams, which also have been proposed to collect IDPs. The chemical analysis data and chromatograms were obtained using the Dynamic Headspace GC/MS method discussed in Section 2.1. The results are exploratory in nature because financial constraints prevented obtaining sufficient data to allow rigorous comparisons and evaluations of the influence of process variables on subsequent aerogel purity.

### 2.3.1 Aerogel Processing Impurities

Impurities in the aerogel products may have resulted from: (a) initial impurities in the sol-gel precursor chemicals, (b) items used to prepare, contain, and protectively cover the sol-gels, (c) chemical reaction byproducts during gellation, (d) contamination during placement of the methanol immersed sol-gels into the HSES, (e) residual contaminants within the High temperature Solvent Extraction System (HSES) itself, and (f) chemical reactions during supercritical extraction. Impurities from the precursor chemicals, during sol-gel preparation, and placement into the HSES were controlled using the procedures described in Section 2.2. Chemical reaction byproducts formed during gellation should have been removed with the extracted methanol because it is believed that most if not all of the organic and organosilane byproducts are soluble in methanol. Residual impurities in the HSES from its construction were reduced by cleaning the system and conducting several runs prior to producing aerogel for this study. Chemical analysis of those early runs, with and without aerogel, showed that, after the first few runs, the HSES itself did not significantly add to the contamination of the aerogel. Analysis of the extracted methanol showed that byproducts produced during gellation or during supercritical extraction were, in fact, removed during the extraction process along with the methanol. Residual impurities in the final aerogel product were further reduced by a final bake-cleaning of the product, as described in Section 2.2. Based on technical experience, we doubt that significant impurities remained chemically bound to the final aerogel product and thus were not undetected by the DH/GC/MS method. However, the analysis study required to prove this assertion was not conducted due to program financial constraints. Chemical analysis showed that highly pure aerogel was produced with residual impurities having concentrations < 0.5 ppm.

### 2.3.2 Aerogel Purity

The data on aerogel product purity are presented in chromatographs and in tables. In the chromatographs, the total outgas mass spectrometer ions detected is plotted with respect to time, given in digital form as Scan Number and in minutes:seconds. The tables list the detected outgas mass associated with the chromatograph peaks along with the name of the identified materials

(Probable Compounds), if possible, and, in some cases, with respect to the digital scan number at the peaks. In the tables, if detected outgas mass is given it is shown as Weight Material Outgas while concentration is given as Weight/Weight in parts per million (ppm), and sometimes also in mg/mg and in Weight/Volume. Digital time scan numbers were obtained for masses from 20 amu to 500 amu. This range includes most low molecular organics, but excludes water, methane, and other very low molecular weight organics, as discussed in Section 2.1. A large peak occurs in each chromatogram due to the CO<sub>2</sub> found in the room air. The peak for CO<sub>2</sub> also is listed in the tables. The sensitivity of the DH/GC/MS analysis method was increased as the aerogel purity improved during the course of the program. This resulted in a corresponding decrease in the minimum detection limit for the outgas mass. As described in Section 2.1, MDLs initially were about 1 ppm for aerogels produced early in the program while for the aerogels produced later the MDL was lowered to approximately 0.01 ppm.

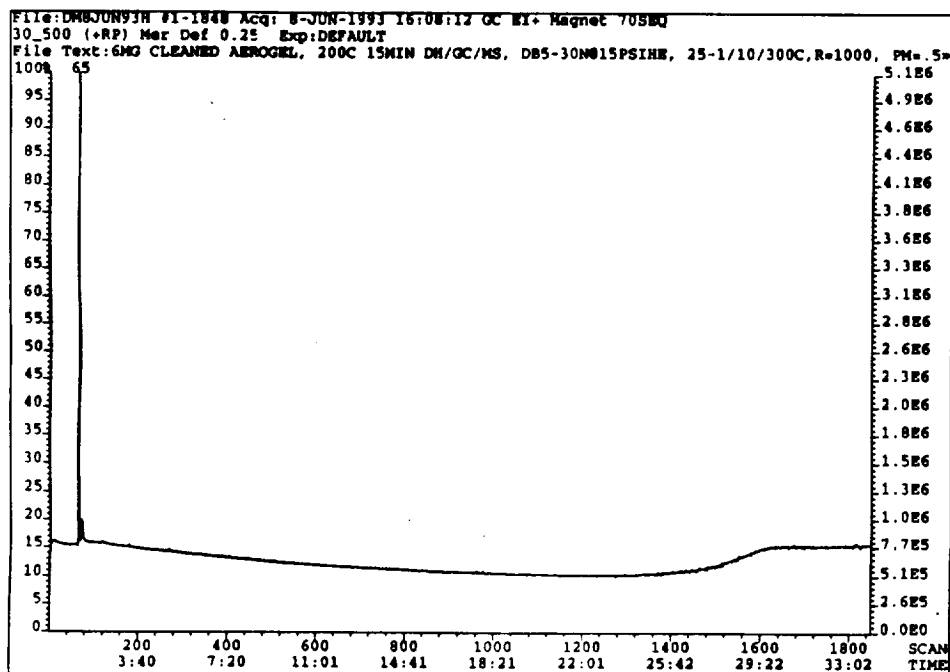
The procedures described in Section 2.2 to manufacture aerogel were expected to produce aerogel products with two different purity levels: "nominal" and "high-purity." Nominal aerogel was produced with a catalyst while "high-purity" aerogel was produced without a catalyst and with the specially prepared precursor chemicals and associated procedures for making the sol-gel described in Section 2.2. To obtain the highest purity, many aerogels were subjected to a bake "cleaning" procedure also described in Section 2.2. The various aerogels produced are thus identified here as: LM "Nominal" Aerogel, LM Clean "Nominal" Aerogel, LM "High-Purity" Aerogel, and LM Clean "High-Purity" Aerogel.

Figure 2.3-1 shows the chromatograph for aerogel produced early in the program by "high-purity" methods followed by a 1 hr bake cleaning. The MDL of the analysis was 1 ppm. No table is included since the only peaks are those for CO<sub>2</sub>, an aliphatic ester artifact accidentally introduced during the analysis, and residual methanol. Figure 2.3-1 shows that to an MDL of 1 ppm that the "high-purity" manufacturing method plus bake cleaning for 1 hour (small samples in stainless steel tube with O<sub>2</sub>) produced a highly pure aerogel product. Any individual impurity was less than 1 ppm.

**Figure 2.3-1 Chromatograph of LM Clean "High-Purity" Aerogel  
Produced in June 1993**

Sample Weight = 6.0 mg, MDL = 1 ppm

**Chromatogram of Cleaned (350C/O<sub>2</sub>/1hr) Aerogel, 6 mg, 200C 15 min DH/GC/MS.**



As aerogel manufacture techniques improved during the program, resultant aerogel product purity increased. Typical aerogel purity level achieved using the "high-purity" procedures later in the program is given in Table 2.3-1. Corresponding chromatograms are given in Figures 2.3-2A and B for the before and after cleaning conditions. The MDL for these data was 0.01 ppm. After bake cleaning, no individual impurity exceeded 0.37 ppm and total residual impurities other, than methanol, were less than 1.5 ppm. The beneficial effect of the "cleaning" process is clear in the table and figures which show that residual methanol was reduced and total other impurities were reduced from approximately 4.5 ppm to less than 1.5 ppm. Some impurities appeared to somewhat increase but this is believed to be an artifact of variations in impurities within different samples.

Table 2.3-2 shows LM "Nominal" Aerogel and LM Clean "Nominal" Aerogel (20 hours bake cleaning) produced late in the program (fall 1994). The methanol content was higher than expected due to some extraction procedural changes made at the time. The HSES extraction procedure subsequently was changed to more effectively purge the extracted methanol. Note, however, in the tables and chromatographs that the impurities in the LM "Nominal" Aerogel, besides the residual methanol and other alcohols, were all quite low, usually less than 1 ppm. Subsequent bake cleaning reduced all of the residual impurities to less than the MDL of 0.01 ppm except for the dibutyl phthalate (a common industrial contaminant) detected at the 0.1 ppm level.

Although the residual methanol was quite high in the LM "Nominal" Aerogel or LM Clean "Nominal" Aerogel of Table 2.3-2, the other impurities were essentially as low as or lower than that detected in the LM "Ultra-Pure" Aerogel or LM Clean "Ultra-Pure" Aerogel (compare Tables 2.3-1 and 2.3-2). As a consequence, all aerogels produced after November 1994 through the end of the laboratory work on the program (June 1995) were manufactured using the "Nominal" procedures described in Section 2.2. The bake cleaned "nominal" produced aerogel continued to have low impurities ( $< 1$  ppm) except in those cases where impurities were accidentally introduced during handling after manufacture was complete as described in Section 5. The changes in the HSES procedure, referred to above, greatly reduced the residual methanol in the product, but not to the level achieved when "high-purity" procedures were used. The higher residual methanol content in the LM "Nominal" Aerogels as compared to the LM "High-Purity" Aerogels is speculated to be due to two possibilities: (1) an unidentified change in HSES extraction procedure that occurred due to a operator personnel change that occurred in late 1994 or (2) the LM "High-Purity" Aerogels having a smaller aerogel particle size and different pore size then the LM "Nominal" Aerogels allowing an easier removal of the methanol during HSES extraction and subsequent bake cleaning. Due to financial limitations, neither of these possibilities was further explored.

**Comparison to "Commercial" Aerogels and to Foams:** Table 2.3-3 lists the residual impurities of a "commercially" produced aerogels available at the time which was considered to be pure, obtained from other sources. The chromatograph of the "commercial" aerogel is shown in Figure 2.3-4. A comparison of Tables 2.3-1 and 2.3-2 with Table 2.3-3 shows that the LM Clean "Nominal" and "High-Purity" Aerogels produced in this program contained approximately three orders of magnitude less residual impurities than the "commercial" aerogel when methanol is excluded and two orders of magnitude less residual impurities when methanol is included. Table 2.3-4 shows a qualitative comparison of the LM Clean "High-Purity" Aerogels from this study compared to other aerogels and to foams which also have been proposed to collect IDPs. The purity of the LM Aerogels is much better than the foams which contain many contaminants at high concentrations that could mask molecules of interest to the investigation of IDPs for the exobiology mission needs as previously stated.

**Table 2.3-1 Example of Purity Levels of LM “High-Purity” and LM Clean “High-Purity” Aerogel Produced in May-November 1994**

Sample Weights = 10.5 mg &amp; 5.80 mg, MDL = 0.01 ppm

LM “High-Purity” Aerogel Impurity Concentration, ppm (µg/g)	LM Clean “High-Purity” Aerogel Impurity Concentration, ppm (µg/g)	Probable Compound
		carbon dioxide (Artifact)
0.26		methyl chloride
33.51	3.78	methanol
0.13		trimethylfluoro silane
0.25	0.32	acetone
0.15	0.37	carbon disulfide
0.22		methoxytrimethyl silane
0.44		trimethyl silanol
0.07		hexane
0.72		methyl ethyl ketone
0.08	0.13	tetrahydrofuran
0.08	0.04	benzene
0.03	0.02	unknown hydrocarbon
0.03		unknown hydrocarbon
0.08	0.01	toluene
0.07	0.08	unknown hydrocarbon
0.24	0.01	hexamethyl cyclotrisiloxane
0.03		methyl cyclopentanone
0.03		unknown hydrocarbon
0.03		unknown hydrocarbon
0.17	0.03	octamethyl cyclotetrasiloxane
	0.07	oxtenal
0.04		aliphatic ketone
0.07		eucalyptol
0.03		unknown hydrocarbon
0.08		aldehyde
0.17	0.19	decamethyl cyclopentasiloxane
0.03		nonane
0.06	0.02	dodecamethyl cyclohexasiloxane
0.08		unknown hydrocarbon
0.06		aliphatic hydrocarbon
0.12	0.10	diethyl phthalate
0.02		unknown hydrocarbon
0.03		unknown hydrocarbon
0.12		dibutyl phthalate
Total 38	5.2	
Total 33.5	3.78	methanol
Total 4.5	1.42	other contaminants

\* Calibrated externally on methyl ethyl ketone, 1µl in CCl<sub>4</sub> at 1:10,000 v/v, n=3 standard runs; blank corrected.



**Figure 2.3-2A Chromatograph of Example LM "High-Purity" Aerogel Produced in May-November 1994**

Sample Weight = 10.5 mg, MDL = 0.01 ppm

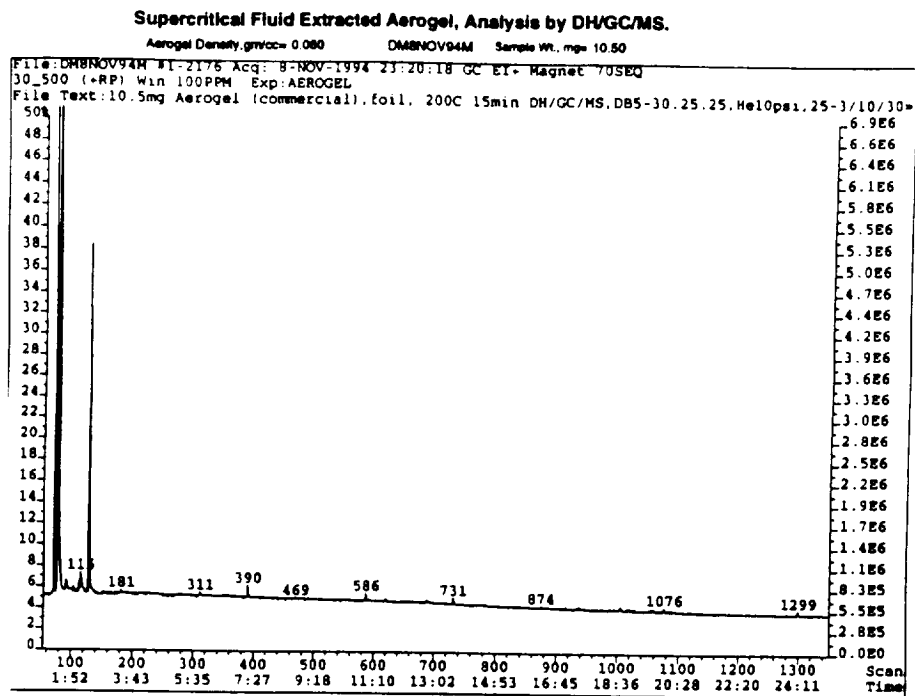


**Figure 2.3-2B Chromatograph of Example LM Clean "High-Purity" Aerogel Produced in May-November 1994**

Sample Weight = 5.8 mg, MDL = 0.01 ppm

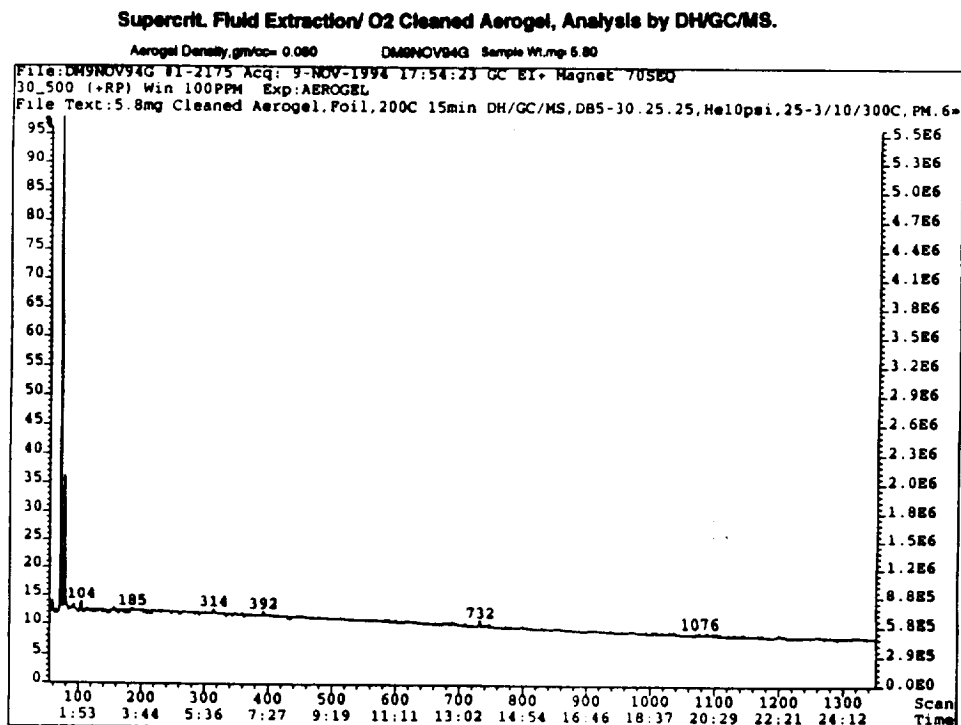


**Table 2.3-2 Example of Purity Levels of LM "Nominal" and LM Clean "Nominal" Aerogel Produced in November-December 1994**

Sample Weights = 9.50 mg & 9.40 mg, MDL = 0.01 ppm

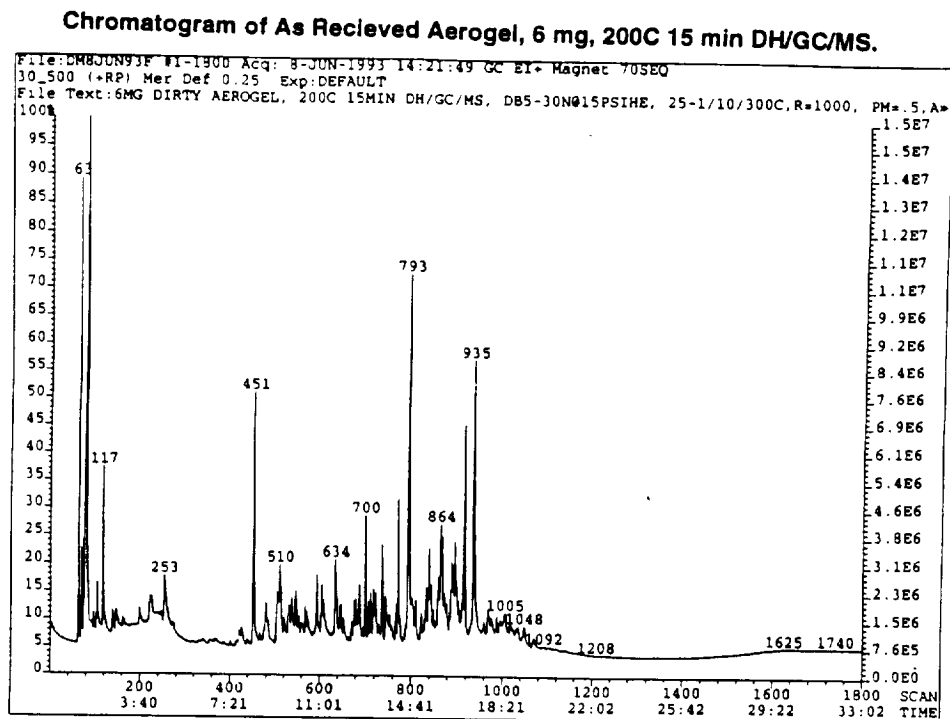
LM "Nominal" Aerogel Impurity Concentration, ppm (µg/g)	LM Clean "Nominal" Aerogel Impurity Concentration, ppm (µg/g)	Probable Compound
		carbon dioxide (Artifact)
617	86	methanol
1.04		acetone
0.66		unknown alcohol
0.09		2-methyl-4,5-dihydrofuran
0.08		1-methylbutyl acetate
0.12		glycerol, dimethyl ether
13		2-butoxyethanol
0.14		1-butoxy-2-propanol
0.07		unknown aliphatic alcohol/ether
0.07		unknown hydrocarbon
0.11		decane isomer
0.11		octamethyl cyclotetrasiloxane
0.10		aliphatic aldehyde
0.06		aliphatic ester
0.06		eucalyptol (cineole)
1.46		aliphatic alcohol/ether
0.04		aliphatic alcohol
0.16		aliphatic aldehyde
0.03		norinone isomer
0.02		camphor
0.64		decamethyl cyclopentasiloxane
0.06		aliphatic aldehyde
0.05		aliphatic hydrocarbon
0.07		dodecamethyl cyclohexasiloxane
0.11		tetradecane
0.04		aliphatic ketone
0.19		pentadecane
0.13		hexadecane
0.11		aliphatic diester
0.10		diethyl phthalate
0.06		aliphatic hydrocarbon
0.11		heptadecane
0.06		aliphatic hydrocarbon
0.06		aromatic compound
0.05		octadecane
0.17	0.14	dibutyl phthalate
Total 637	86.14	
Total 617	86	methanol
Total 20	0.14	other contaminants

\* Calibrated externally on methyl ethyl ketone, 1µl in CCl<sub>4</sub> at 1:10,000 v/v, n=3 standard runs; blank corrected.

**Table 2.3-3 Residual Impurities Found in "Commercial" Aerogel**

Sample Weight = 6.00 mg, MDL = 1.0 ppm

Scan Number	Impurity Concentration, ppm ( $\mu\text{g/gm}$ )	Probable Compound
63		CO <sub>2</sub> artifact
70	27	methanol
74	28	ethanol
77	70	acetone
79	130	isopropanol
104	17	methyl ethyl ketone
117	30	tetrahydrofuran
146	14	1-butanol
253	42	hexanal
451	88	octamethylcyclotetrasiloxane
479	30	trimethyl benzene
504	20	methyl propyl benzene isomer
510	53	methyl propyl benzene isomer
531	17	dimethyl ethyl benzene isomer
537	20	methyl propyl benzene isomer
546	18	undecane
571	15	tetramethylbenzene isomer
593	25	decamethylcyclopentasiloxane
604	14	branched hydrocarbon
607	27	branched hydrocarbon
634	42	dodecane
646	19	tridecane
679	14	tetradecane isomer
687	25	tetradecane isomer
700	34	pentadecane isomer
711	13	tetradecane isomer
717	18	pentadecane isomer
722	18	cyclic pentadecane isomer
736	30	pentadecane isomer
767	12	branched hydrocarbon
771	51	branched hydrocarbon
793	163	branched hydrocarbon
801	33	branched hydrocarbon
810	19	branched hydrocarbon
832	26	hexadecane isomer
839	46	hexadecane isomer
843	16	branched hydrocarbon
859	28	cyclic heptadecane isomer
864	38	branched hydrocarbon
867	34	heptadecane isomer
871	22	branched hydrocarbon
888	25	branched hydrocarbon
892	22	heptadecane isomer
895	21	octadecane isomer
899	16	branched hydrocarbon
912	18	branched hydrocarbon
916	71	branched hydrocarbon
935	116	branched hydrocarbon
968	15	cyclic octadecane isomer
total =	1,690	

**Figure 2.3-4 Chromatograph of "Commercial" Aerogel****Table 2.3-4 Qualitative Comparison of the LM Clean High-Purity Aerogel to Other Aerogels and to Foams**

Material	Major Constituent (1-10% wt./wt.)	Minor Constituent (0.1-1.0% wt./wt.)	Trace Constituent (1-1000 ppm)
LM Clean "High Purity" Aerogel O2/350C/1 hr	NONE	NONE	NONE (except methanol)
Medium Blue Foam	styrene	Cl-benzene, propylbenzene Br-benzene, BrCl-benzene diBr-benzene, styrene dimer phenyl-naphthalene	MANY
Gray Foam	butyl amine isomer?	benzaldehyde phenyl-naphthalene	SEVERAL
Powder Blue Foam	styrene, Cl-benzene Br-benzene, BrCl-benzene diBr-benzene, styrene dimer phenyl-naphthalene	benzene, xylene, propyl and methylethyl benzenes diCl-benzene, Br-Cl-benzene other polyhalo-benzenes	MANY
Yellow Foam	trichlorofluoromethane	NONE	MANY
Gray Foam	NONE	NONE	MANY
White Foam	isopentane, styrene isopropyl benzene styrene dimer phenyl-naphthalene	pentane isomers xylene, benzaldehyde acetophenone styrene dimer	SEVERAL

## 2.4 AEROGEL OPTICAL TRANSMISSIVITY

The optical transmissivity or clarity of silica aerogels is one of its defining characteristics. Together with the extremely low density, the clarity of aerogel has given rise to its nickname: "solid smoke". Aerogel clarity is a key issue for its use as an IDP capture medium. Location, identification and extraction of particles and particle tracks is a central part of an overall investigative plan. Aerogel should be sufficiently transparent to facilitate this objective. Additionally, optical transmissivity itself may serve as a valuable quality assessment tool, providing an indication of density uniformity and cleanliness (chemical purity). Optical clarity also is the single most important feature of aerogel synthesized for Čerenkov radiation detectors in the high-energy physics community. Physicists rank the value or quality of an aerogel product exclusively by this single factor.

### 2.4.1 Transmissivity Measurement and Data Analysis

Optical transmissivity was measured with a Cary Model 219 Spectrophotometer. This unit allowed probing of the optical transmissivity of a specimen over a wavelength range of 187 to 875 nm. Radiation wavelengths were selected at 1 nm intervals. The monochromatic radiation beam is split into two, one directed through the specimen and one used as a reference and directed through "open space" within the specimen cavity. Both beams converge on a photodetector, their intensities are compared, and the difference is recorded as the optical transmittance for that particular wavelength.

When transmittance data has been collected for all wavelength of interest, a plot is prepared of transmittance (%) vs. wavelength (nm). For the case of aerogel, this plot is unique to a specified density, thickness, and overall specimen quality. By "quality" we mean the processing variables that affect transmissivity - including chemical purity, surface-absorbed contamination, absorbed moisture, or aerogel crystallite size. To compare and rank the "quality" for a variety of aerogels, further analysis is required. To compare the quality of two aerogels requires that the variables of density and thickness be fixed. Thickness can be normalized analytically through consideration of the Rayleigh scattering equation:

$$T = A \exp (-CL/\lambda^4)$$

T is Optical Transmissivity

A is Saturation Transmissivity at 800-900 nm

L is the aerogel thickness in cm

l is the radiation wavelength in  $\mu\text{m}$

C is the Rayleigh Scattering Coefficient in  $\mu\text{m}^4\text{cm}^{-1}$

On a plot of percent transmissivity against the fourth power of the inverse radiation wavelength, the slope corresponds to the quantity  $CL$ . By dividing out the thickness  $L$ , one arrives at a value for the Rayleigh scattering coefficient  $C$ . For the range of aerogels produced in the world today, a value of  $C = 0.0100 \mu\text{m}^4\text{cm}^{-1}$  for densities near  $0.050 \text{ g/cm}^3$  is considered to be of extremely high quality.

Optical transmissivity is a useful technique both as an in-house quality control tool as well as to document that the as delivered aerogel meets the agreed upon specification. Comparison of two aerogels can only be a fair comparison if the densities are the same and the thickness has been normalized (analytically) to 1 cm.

### 2.4.2 Factors Expected to Influence Optical Transmissivity

Aerogel transmissivity is influenced by a number of factors.

- Density Less dense aerogels have greater optical transmissivity because the distance between  $\text{SiO}_2$  particles is larger and the number of particles is less.

- **Thickness** Thinner aerogels appear to be clearer because there is less material through which photons transit and can be absorbed.
- **Chemical Purity** Chemical impurities will exhibit a "signature" absorption behavior at selected wavelengths and decrease the overall aerogel transmissivity.
- **Aerogel Synthesis Practice** Crystallite size in the aerogel body is expected to be amenable to experimental control through factors such as gellation time (controlled by catalyst content), gellation temperature, and density. The crystallite size, in turn will affect the optical transmissivity. Experiments to date at Lockheed have not assessed this factor in a quantitative manner.
- **Aerogel Aging Practice** During the gelling stage of aerogel synthesis, several byproducts are produced. These organics and organosilanes are soluble in methanol - the medium used to age the gel prior to supercritical extraction. By frequently changing the aging bath to "fresh" methanol, the concentration of these chemical byproducts is made progressively more dilute and the resultant aerogel clarity is expected to improve. However, the cost of the product will increase because removing the byproducts from the methanol is difficult. Experiments to date at Lockheed have not assessed this factor in a quantitative manner.
- **Supercritical Extraction** It has been our observation that control of the chamber atmosphere during the final cooling stage of the supercritical extraction sequence is critical to achieving high aerogel clarity. At room temperature, if a piece of aerogel is placed into contact with methanol, the aerogel is attacked and destroyed. Consider the final stages of the supercritical extraction process: As the chamber pressure is lowered to ambient room pressure, the chamber temperature is maintained at about 330°C. At this point, the atmosphere above the aerogel consists of a cloud of pure methanol vapor at 1 atm pressure. When the temperature is reduced, this methanol vapor can condense onto the aerogel rendering the aerogel basically unusable. To mitigate this effect, flowing argon is used to continuously purge the process vessel during the cooling cycle. In this way, the methanol vapor is displaced resulting in a highly transmissive product.
- **Post-Processing** Other factors, such as bake-out treatments and absorption of humidity from the ambient air, are expected to affect the transmissivity of aerogel. These factors have not been studied extensively at Lockheed Martin, however, some transmissivity data is presented below that explores some of the factors to a limited extent.

### 2.4.3 Observations Regarding LMSC Aerogel Transmissivity

Aerogel product prepared for the ACCs, described in detail in Chapter 5, was examined for optical transmissivity. The physical parameters of this material were: thickness of 1.5 cm, density of 0.060 g/cm<sup>3</sup>, and index of refraction of 1.016. The transmissivity of this aerogel was measured under three conditions:

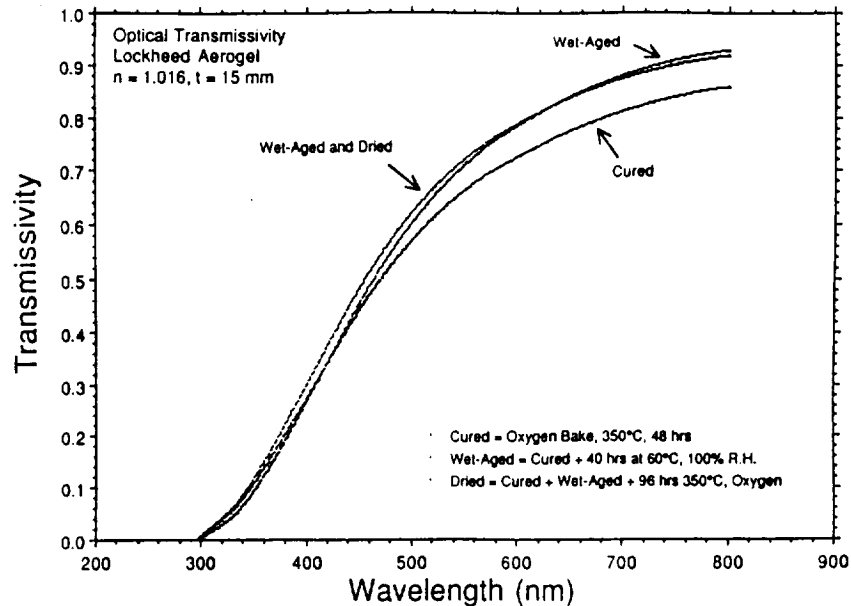
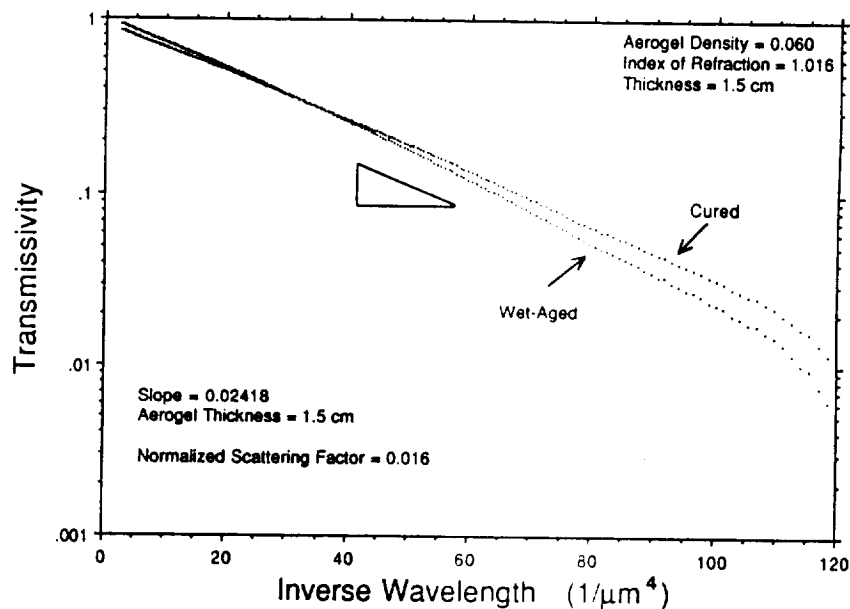
"Cured" As-extracted and baked in oxygen, 350°C, 48 hr.

"Wet-Aged" Cured + 40 hr. at 60°C, 100% Relative Humidity

"Dried" Cured + Wet Aged + 96 hr. 350°C Oxygen Bake

The transmissivity results for these three cases are shown in Figure 2.4.3.1 below. These results show that the "Wet-Aged" and the "Dried" conditions had better overall transmissivity than the "cured" condition. This result is unexpected since conventional wisdom holds that aerogel "cloudiness" is attributable to absorbed moisture. Clearly, further exploration of this area is required to fully understand processing and storage variables that can affect aerogel transmissivity.

The Rayleigh Scattering Coefficient was determined for these materials and is summarized in Figure 2.4.3.2. The slope of these data are similar for the two cases shown, resulting in a scattering coefficient of  $C = 0.0160 \mu\text{m}^4\text{cm}^{-1}$ . This value for the scattering coefficient  $C$  is indicative of a good level of transmissivity.

**Figure 2.4.3-1 Optical Transmissivity data for ACC-Quality Aerogel****Figure 2.4.3-2 Rayleigh Scattering Parameter Analysis**

A number of research questions related to transmissivity were not investigated due to funding restrictions. The effects on optical transmissivity of long term aging, aerogel spatial uniformity, and manufacturing processing variables remain to be determined. For aerogel being subjected to long term aging, there are issues such as: does the aerogel become more cloudy with time, can the cloudiness be reversed (by bake cleaning, for example), what is the cause of cloudiness if it occurs (exposure to light, absorption of moisture, etc.). The effect of processing variable include not only the effects of impurities, but also such variables gelling time and extraction procedures. Finally, transmissivity also may be affected by the aerogel cell and particle size. The effect of all of these variables on transmissivity remain to be investigated.

## SECTION 3.0

### CONTAMINATION ENTRAINMENT

For an IDP capture mission, the capture media should initially be as pristine as possible and should remain so throughout the launch and recovery phase. However, organic contamination is known to exist around space platforms. On Shuttle or Mir type human occupied platforms, the contamination primarily comes from the human waste disposal systems, but also from the propulsion systems and the platform structure (such as outgassing). On the shuttle, contamination also comes from the non-organic debris associated with the interior of the shuttle bay. Other unmanned space platforms also give off contaminants, especially from their propulsion systems and through outgassing. Thus, exposure of the capture media could be in an environment which may have organic or inorganic material which could deposit themselves on the capture media surface.

If contamination on the surface of an ACC would contaminate both the impacting particle and the resultant track during an impact event, the naturally occurring organics of a captured IDP could be masked. Therefore, experiments were conducted to evaluate (1) whether surface contaminants survive the impact process and if they are entrained in the track made by an impacting particle, (2) whether the surface contaminants would enter the aerogel/particle track after particle capture, (3) the potential diffusion of surface contaminants into aerogel over a 180 day period; and (4) the potential for post-impact contaminants diffusing along the track boundaries into the aerogel thus potentially contaminating other tracks and captured particles. Glycine, a known, easily identified, organic tracer was used to represent surface contamination. Glycine was selected because it (1) is a relatively simple organic molecule, (2) is absent in the HVGR, and (3) is not used in aerogel manufacture.

#### 3.1 EXPERIMENTAL CONDITIONS

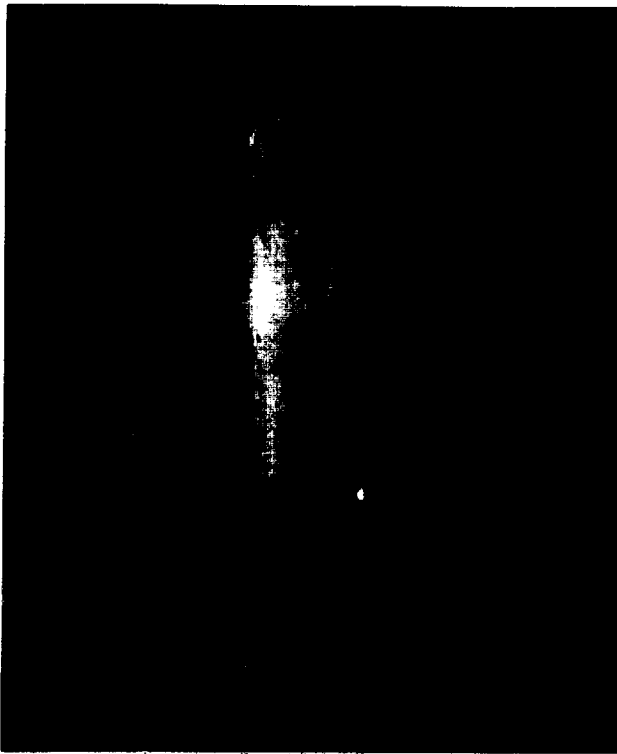
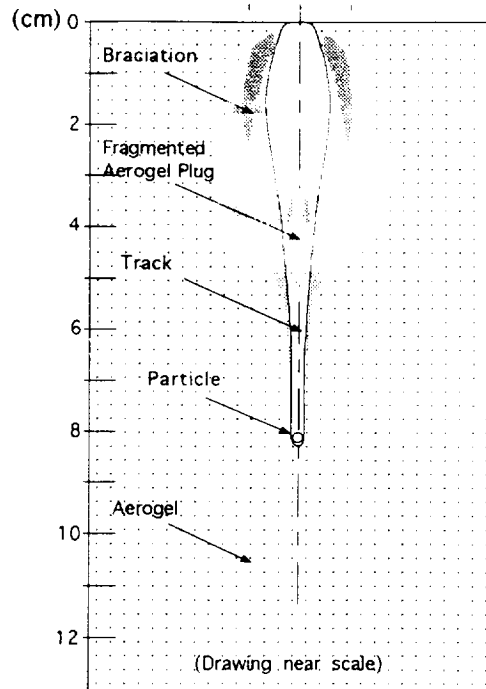
Three cylindrical aerogel ingots approximately 14.0 cm in diameter and 12 cm in length with a density of approximately 61 mg/cc were prepared for the experiments using the methods described in Section 2.2. The resulting ingots had the same type of contamination as that described in Section with all contaminants being less than 1 ppm, exclusive of residual. Subsequent chemical analysis showed that any initial glycine, exclusive of that deliberately applied to the top surface, was less than the MDL level of 12 ppb. The aerogel ingots were cast in a low melting temperature metal in an argon inert atmosphere and surface coated with the glycine "contaminants."

#### 3.2 EXPERIMENTAL RESULTS

##### 3.2.1 Organic Entrainment

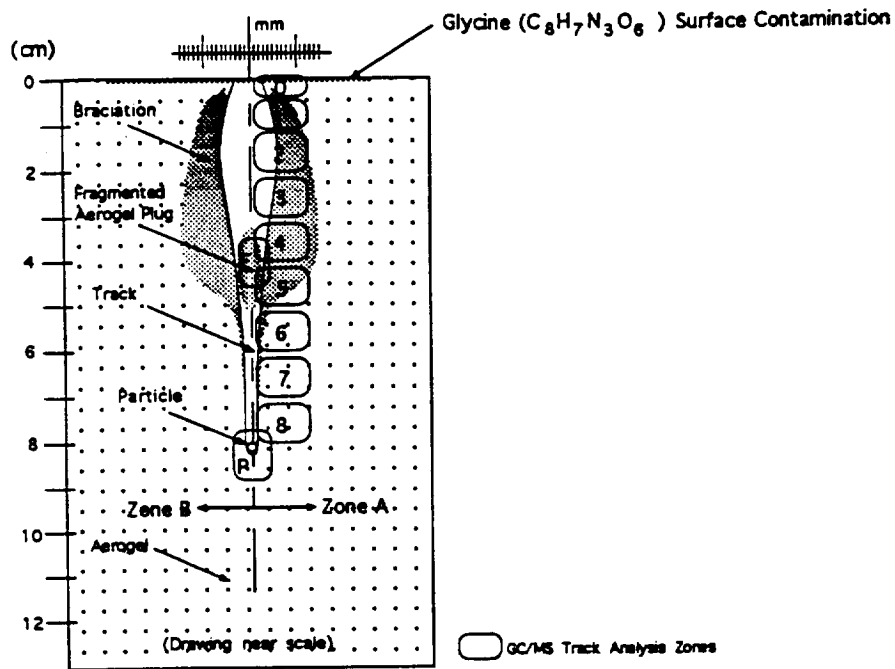
One aerogel ingot was used to evaluate (1) whether surface contaminants survive the impact process and if they are entrained in the track made by an impacting particle, (2) whether the surface contaminants would enter the aerogel/particle track after particle capture. The ingot was cooled to 79° K and subjected to an impacting Carnelian particle (0.001 gm mass) with 6.6 joules kinetic energy (3.6 Km/sec velocity). In the Phase I Final Report, the details of this experiment along with schematics and pictures are given in Section 4 as the LS4-8 experiment. The resulting 8.2 cm track was analyzed for the presence of the organic contaminant at various depths. The track characteristics of the particle captured in this experiment were used as the primary input to the additional analysis conducted with the CTH model whose results are given in Section 3. The track and diagram are shown in Figure 3.2.1-1.



**Figure 3.2.1-1 Picture and Diagram of Track for LS4-8****LS4-8 Aerogel Ingot****Diagram of Track in LS4-8**

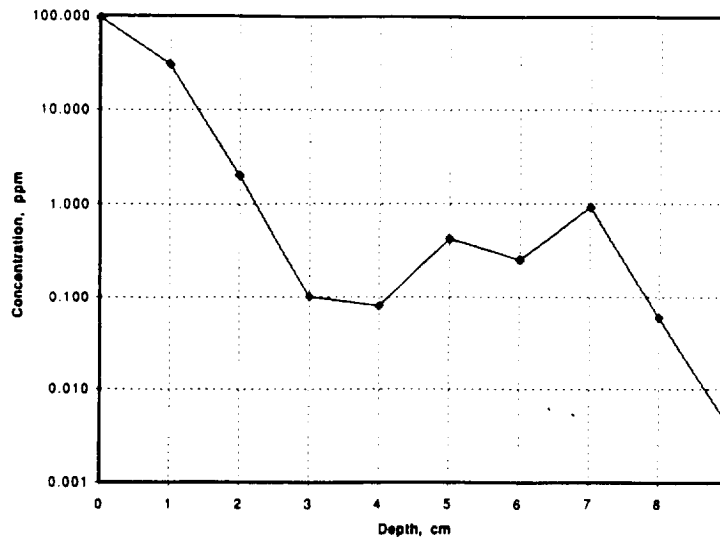
After particle impact, the front surface of the aerogel ingot was placed in a face-down orientation and then carefully removed. This orientation reduced the possibility of track contamination being caused by the surface material falling into the track channel. The aerogel ingot was divided along the track itself. The particle fell out into a waiting beaker. The two halves were isolated in two separate beakers in a "track-exposed-face-up" orientation so that any contamination would not fall into the track and so that the "bottom-up" track separation process could be initiated minimizing any contamination which might fall into a lower zone. Both the left and right side of track was divided into subsections. The subsections from one side were examined using the GC/MS for analyzing Glycine described in Section 4. . Figure 3.2.1-2 illustrates the volume elements which were tested for glycine. Section A0 included the surface of the aerogel "contaminate" with glycine and the first approximately 2 millimeters of aerogel below the surface. Section A1 included the aerogel below the A0 section down to a 1 cm depth. Sections A2 through A8 included the aerogel from below Section A1 down to a 2 cm depth, Section A3 from below Section A2 down to a 3 cm depth, etc. The chemical analysis results are shown in Table 3.2.1-1 and in Figure 3.2.1-3. The MDL for the glycine analysis in this experiment was 0.012 ppm (12 ppb) as discussed in Section 4. The penetration orifice of the track contained many radially oriented, fragile, splinter-like aerogel components. Several of these components had fallen into the track, labeled F in Figure 3.2.1-2, and may have accounted for a significant portion of the low-level glycine concentration shown in Figure 3.2.1-3.

**Figure 3.2.1-2 Volume Elements Along Track of LS4-8 Used for Glycine Analysis**



**Table 3.2.1-1 Glycine Analysis Results for Track of LS4-8**

Aerogel Name	Conc. * (wt/vol) Glycine, gram/cc	Conc.* ppm (wt/wt) Glycine, $\mu\text{g/gram}$
A0	5.8E-6	96
A1	1.8E-6	30
A2	1.2E-7	2.0
A3	5.7E-9	0.10
A4	4.8E-9	0.08
A5	2.6E-8	0.43
A6	1.5E-8	0.25
A7	5.5E-8	0.92
A8	3.5E-9	0.06
F	7.4E-9	0.12
P	2.4E-8	0.39
Extract Blank	2.5E-10	0.004

**Figure 3.2.1-3 Plot of Glycine Analysis Results for Track of LS4-8**

Although the Glycine concentration was much lower after the first 2 cm of track, Glycine was detected along the track, as indicated in Figure 3.2.1-3 and Table 3.2.1-1. The handling procedures, specimen preparation, electrostatic fields created on the surface of the aerogel specimens at the time of preparation, and the aerogel surface around the track cracking off and falling into the track may all have been responsible for the low level of glycine contamination in the track. The penetration orifice contained many radially oriented, fragile, splinter-like aerogel components. Several of these components were observed to have fallen into the track and could have accounted for a significant portion of the low-level glycine concentration shown in Figure 3.2.1-3. The HVGR also has a hydrogen pressure wave which could have forced contaminated aerogel dust into the track. The vibration of the aerogel ingot during handling after the impact test also may have caused surface material to fall into the track. It was not until the ingot was moved to the laboratory, that the ingot was turned on its side to minimize this problem.

### 3.2.2 Contamination Diffusion

Analysis was performed to quantitatively measure the concentration of glycine placed on the surface of the aerogel used in the experiment of Section 3.2.2 after a six month period. A sample was taken from approximately 0.8 to 1.2 cm from the particle surface penetration point and archived. The sample was stored for 180 days in a protected area held at 291K and one-atmosphere of argon. This sample was tested using the GC/MS Glycine analysis method to determine if Glycine was present at several depths below the surface. The results were compared to the initial conditions and, to the sensitivity of the GC/MS method, showed that Glycine was present on the surface in the range of  $0.0001 \text{ g/cm}^2$  at the onset of the test and also at  $0.0001 \text{ g/cm}^2$  at the end of the 180 day waiting period. Measurements also showed no significant penetration of Glycine beyond the surface first 1 mm deep elemental volume. Glycine had not penetrated the surface fissures created by a 003 sanding/polishing. This surface preparation was performed to assure a uniform concentration of the glycine contaminant.

### **3.2.3 Post Launch Organic Diffusion Into Aerogel.**

A portion of the aerogel surface located approximately 1 cm from the track of the particle was preserved intact. This piece of aerogel was cleaved transverse to the track axis and examined using the GC/MS after a 180 day interval. The top surface organic analysis (0 cm to 0.1 cm) showed the expected levels of glycine applied. The second sample consisting of a volumetric zone extending from 1 mm to 1 cm had no measurable glycine. No other non-track samples had any measure of glycine to the limits of the GC/MS. The suggestive entrainment of glycine in the first cm of the track specimens may be explained by aerogel dust contaminated with glycine falling into the track, or simply the very fragile aerogel track penetration orifice edge components may have dislodged and fell into the track.

**3.2.4 Aerogel Surface Debris Removal.** Electron beams, neutral plasmas, and a diverging laser beam were all tried for the removal of embedded carbon on the surface of aerogel. The carbon deposition was produced by launching carbon particles against the aerogel targets at approximately 5 Km/s. Only the laser beam method was successful in removing the surface carbon. Approximately 98% of the deposited carbon particles were removed, leaving only a few agglomerated carbon particle tracks remained embedded below the surface of the aerogel.

## **3.3 CONCLUSIONS**

Evaluation of the contamination levels which could have been caused by a surface contamination due to glycine and entrained in the track of a hypervelocity particle showed Glycine to be detectable within the track. There were no measurable glycine concentrations internal to an aerogel ingot after 180 days of storage.

## SECTION 4

### CTH MODELING OF THE IMPACT PROCESS

The low-density silica based aerogel material is intended to capture cosmic microparticles in a way that preserves both the physical characteristics and size of the particles so that meaningful analysis is possible. In proposed space captures, dust particles can travel at speeds up to 70 km/sec (however the velocity of the platform and Earth can subtract about 40 km/sec). In experimental settings, particle impact velocities are limited by gas gun technology to 10 km/sec. Thus, an analytical tool is needed to model actual hypervelocity dust particle impacts to determine the dimensions of the aerogel material required for capturing cosmic dust particles as well as to evaluate the state of the captured particle.

This section summarizes the results of the work performed to further evaluate the suitability of a particular analytical model, CTH<sup>1</sup> for the prediction of cosmic dust penetration in low density aerogel. The CTH model was used for analyzing high energy particle penetration characteristics into aerogel, as reported in the Phase I Final Report. Based on the results of that work, the model was used to analyze the track characteristics measured in the LS4-8 experiment of Section 2. The CTH model of the Phase I report was initialized and exercised using the parameters of the impact media, aerogel, and particle previously used that provided a reasonable prediction of aerogel performance. However, these parameters were modified based on experimental observations and information obtained from the experiments of Section 2.

The CTH model is a finite volume code developed at Sandia National Laboratories for analyzing high speed impacts. The low-density silica aerogel capturing material is modeled as a two-state material with an initial low density solid state and a second multiphase<sup>2</sup> (crushed) state using the CJ volume burn option in CTH. The CJ volume burn option is an irreversible two-state model with a transition region from the initial to the final state. This model is often used for explosive detonation problems. However, the transition methodology in the CJVB model is applicable for these low density materials where transition from the extremely low density to the crushed material is determined in the model by the material density and the temperature. The use of this model to simulate the impact of microparticles, such as quartz-based materials (Olivine, Carnelian, etc.), into a low-density silica capturing material is described in detail in the Phase I Final Report of this study.

#### 4.1 INITIAL MODELING CONDITIONS

The CTH model was initialized using the parameters of experiment LS4-8, density of 0.061 g/cc and the associated material properties of an carnelian particle of 920  $\mu$  diameter and with a velocity of 3.58 Km/s. The particle tracer locations are defined in Table 4.1-1. At the conclusion of LS4-8, the details of the track characteristics, particle mass, density, and velocity were input to the existing CTH model which had the aerogel's Hugoniot<sup>3</sup> which Sandia Laboratories experimentally determined for an aerogel of 135 mg/cc. Table 4.1-2 summarizes the empirically determined test parameters. Due to an oversight, a density of 0.0648 g/cc was used in the CTH model. The modifications made to the model to achieve a better match of the empirical data are given below.

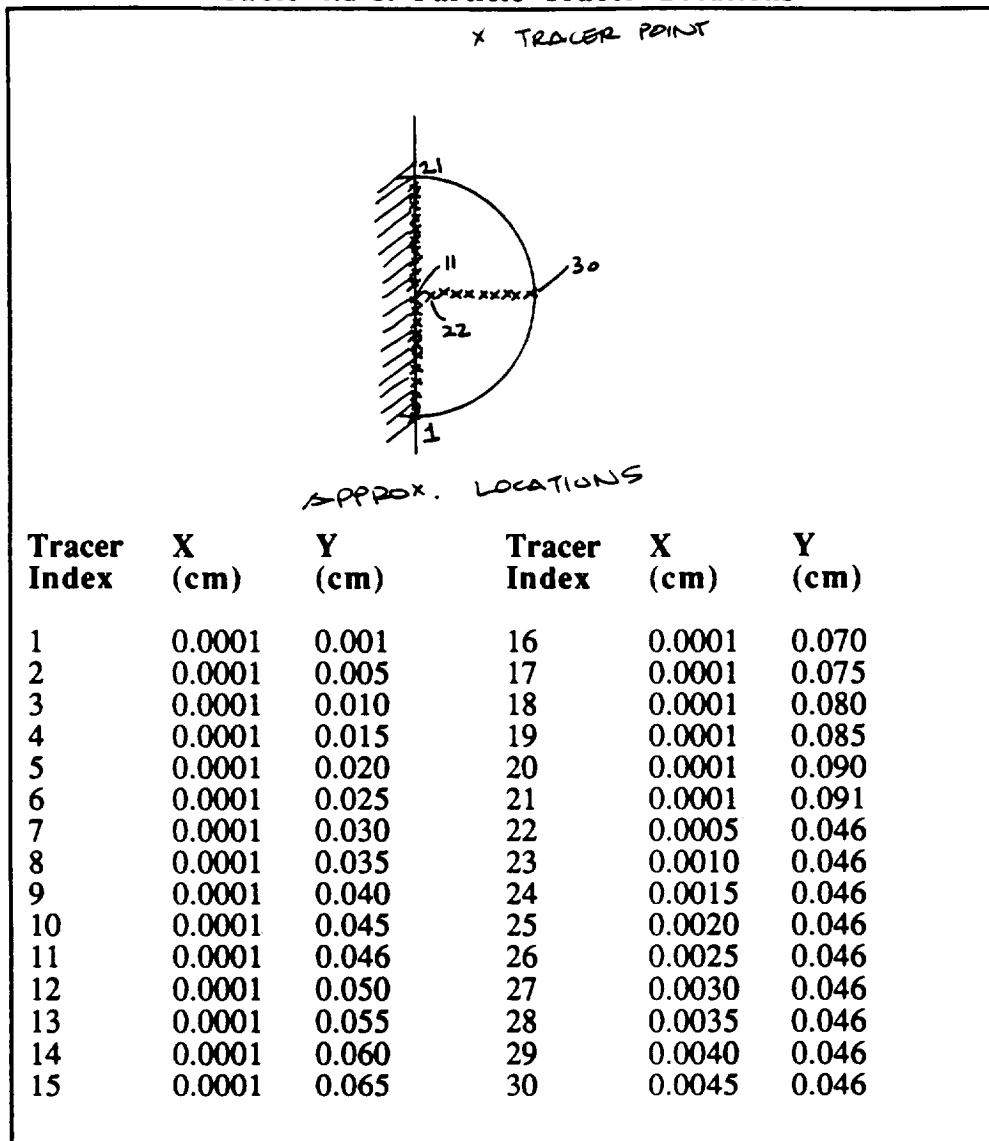
---

<sup>1</sup> Bell, R.L., et al, "CTH User's Manual and Input Instructions", Version 1.026, Sandia National Laboratories, July 1992.

<sup>2</sup> Holmes, N.C., and E.F. See, "Shock Compression of Low-density Microcellular Materials," Shock Compression of Condensed Matter 1991, Schmidt (editor), Elsevier Science Publisher, 1992.

<sup>3</sup> The Hugoniot is simply the physical relationship between the pressure and volume of a material as plotted for the conditions of shock.

Table 4.1-1: Particle Tracer Locations



**Aerogel Capture Media.** Assumptions were made for impact capture media to closely approximate the material properties of aerogel during the impact process.

- a. A tabular material properties table was developed for quartz. The table assumed that the aerogel was immediately crushed during impact to a quartz-like material. This assumption was realistic in that it corresponds to the changes in the BET pore size distribution after aerogel is crushed.
- b. The aerogel was assumed to have an almost zero yield strength during the impact process with a Poisson ratio of 0.4999 to simulate a very soft material with a melt temperature of 1880 K.
- c. A minute fracture stress (0.1 bar) was defined so that tension would not be supported.

**Table 4.1-2: Experimentally Determined Impact Parameters of LS4-8****Aerogel Capture Media:**

- o Density: 0.0648 g/cc
- o Shape: Cylinder: 14 cm Diameter x 12 cm High
- o Impurities:  $\leq 1$  PPM
- o Packaged Method: Fully Encased, Top Exposed.
- o Assumed Temperature: 19°C (actual experiment temperature was 79°K)

**Track Characteristics:**

- o Total Length: 8.25 cm
- o Brachiated 1st 1/2 to 2 cm Diameter
- o Entrance Diameter: 2.7 mm (2.2 to 3.1 mm Star-like shape)

**Projectile:**

- o Carnelian
- o Hardness: 7
- o Mass: 0.00103 g
- o Density: 2.530 g/cc
- o Average Diameter: 0.920 mm
- o Velocity: 3.58 Km/s
- o Kinetic Energy: 6.61 joules
- o Recovery: Intact with Accreted Aerogel

**Carnelian Particle.** Several assumptions were made for the projectile.

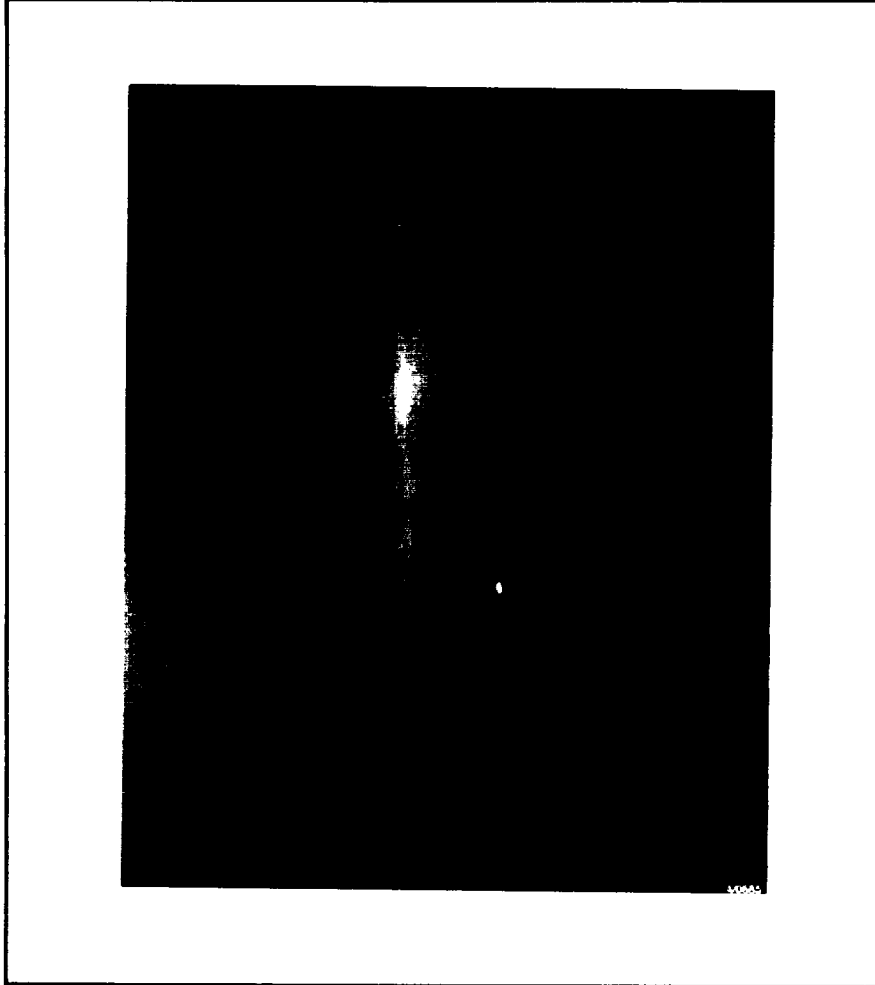
- a. Only the solid quartz linear Us-Up equation-of-state was defined to prevent the particle from experiencing a transition to another state (i.e. to a liquid or vapor).
- b. A very high yield strength ( $98 \cdot 10^{10}$  Pa) and melt temperature (3600 K) was used for the elastic-plastic strength model.
- c. A very high fracture stress ( $1.0 \cdot 10^{10}$  Pa ) was employed to inhibit particle failure.

In addition, the BLINT option<sup>4</sup> that was made available in the latest version of CTH was also exercised as an improved interface logic between the aerogel and the particle

The aerogel track whose parameters are given in Table 4.1-2 is shown in Figure 4.1-1. Figure 4.1-2 is a diagram of the track illustrating several major features which were taken from the aerogel shown in Figure 4.1-1. It should be noted that the track was illuminated in a way to enhance the track and particle. Doing this reduced the overall appearance of its transparency. In addition the photograph was taken with a digital imaging system which further alters the true color. Figure

<sup>4</sup> Silling, S.A., CTH Reference Manual: Boundary Layer Algorithm for Sliding Interfaces in Two Dimensions", SAND93-2487, January 1994.

**Figure 4.1-1: Photograph of a 6.7 Joule Particle Track in Aerogel**

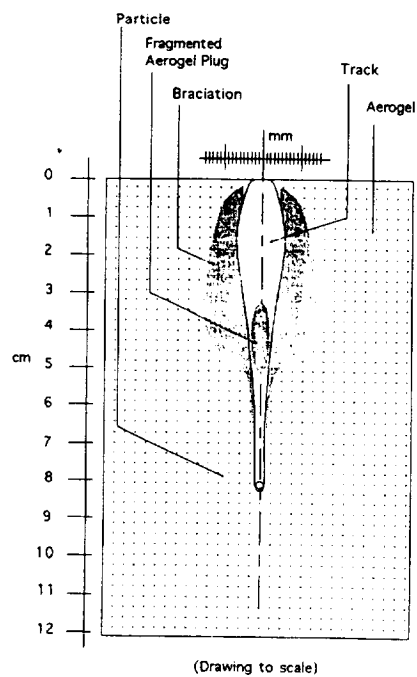


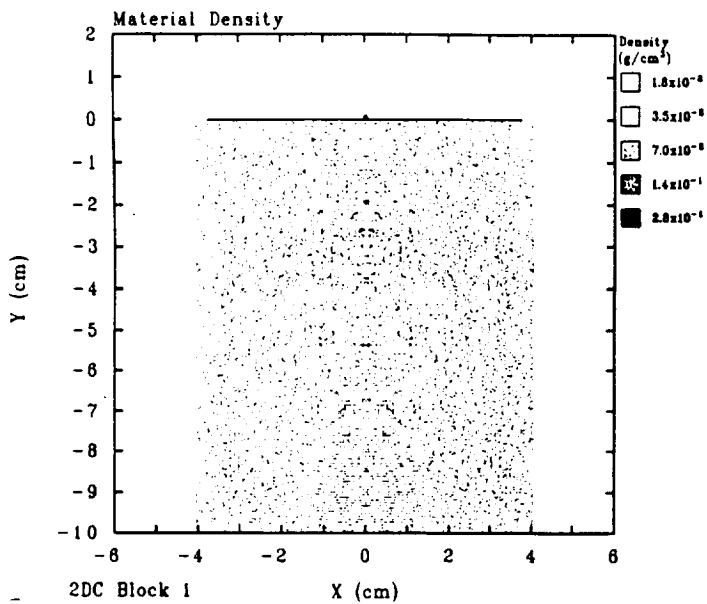
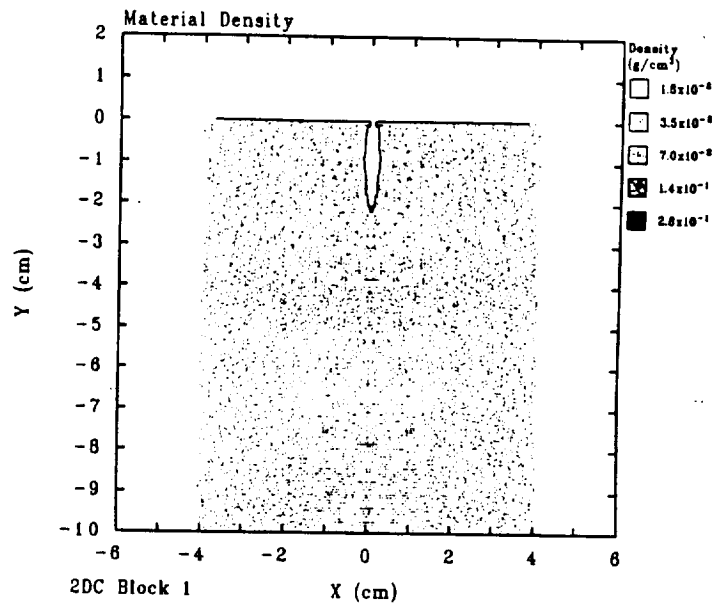
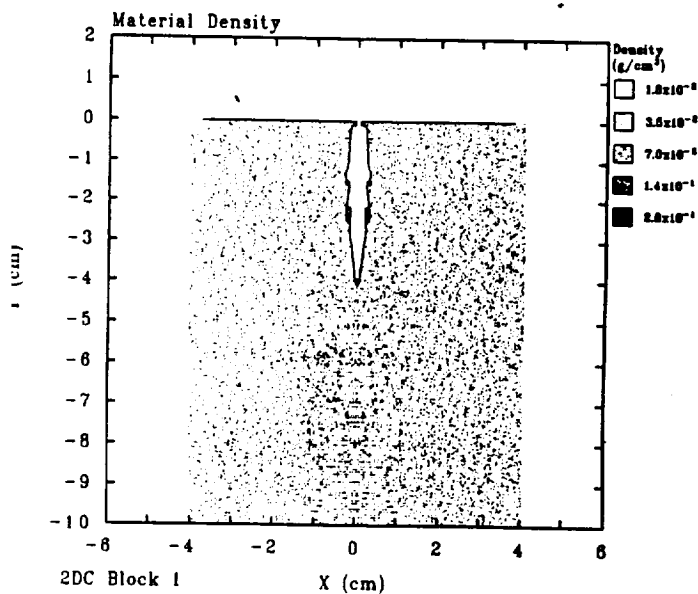
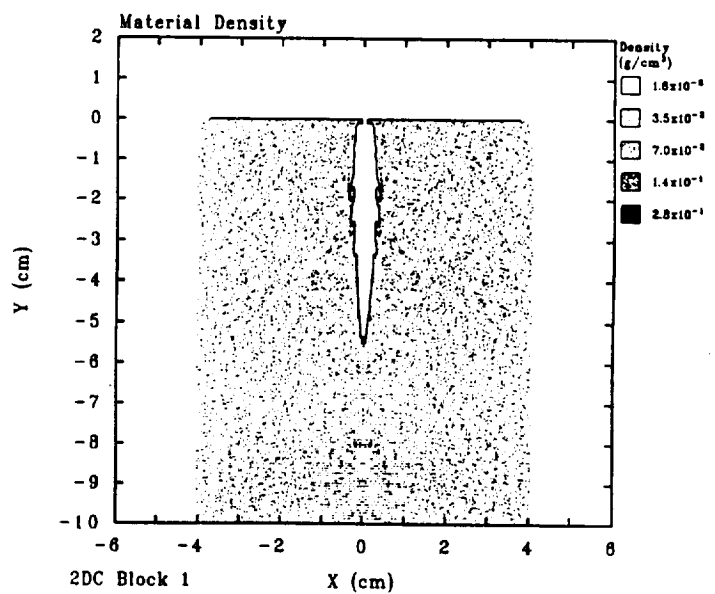
4.1-3 is a close-up of the carmelian particle in the aerogel. With no magnification, it was clearly visible and the accretion of aerogel on the leading edge was likewise visible.

## **4.2 CTH MODELED AEROGEL TRACKS**

Figures 4.2-1 to -4 show the deformation contours of the aerogel and the particle at various times. Although these plots do not show the aerogel fractures along the track, their overall shape conforms very closely to the interior of the aerogel track.



**Figure 4.1-2: Track Diagram****Figure 4.1-3: Carnelian Particle Captured in Aerogel**

**Figure 4.2-1: Aerogel Plot: 0.0 sec.****Figure 4.2-2: Aerogel Plot: 10.0  $\mu$  sec.****Figure 4.2-3: Aerogel Plot: 30.0  $\mu$  sec.****Figure 4.2-4: Aerogel Plot: 55.0  $\mu$  sec.**

### 4.3 OTHER PROFILES

The CTH program provides time histories of particle position, velocity, kinetic energy, and particle interior temperature profiles. These time based plots are shown in Figures 4.3-1 through -4. The deceleration was not provided; however, the velocity profile conforms closely to the expression,

$$Y_t = -3.85 + 20 t^{0.2},$$

with the second derivative as

$$Y_{tt} = 4 t^{-0.8}.$$

This expression numerically is close to that which is obtained using finite differences and it predicts the upper particle deceleration is of order  $10^{10}$  cm/s<sup>2</sup> with corresponding force of  $4 \times 10^4$  dynes, and with a resulting pressure of 440 psi on the particle, assuming a projected surface area facing down.

Figure 4.3-1: Position History.

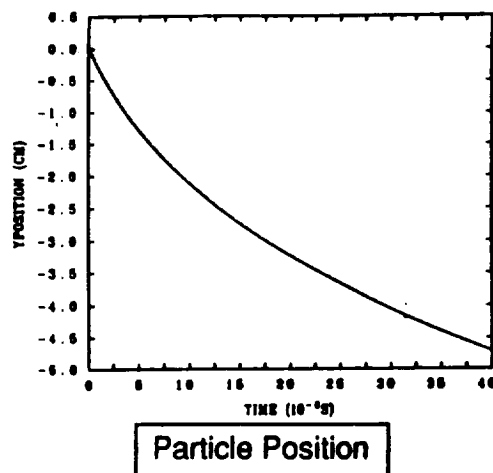


Figure 4.3-2: Velocity History

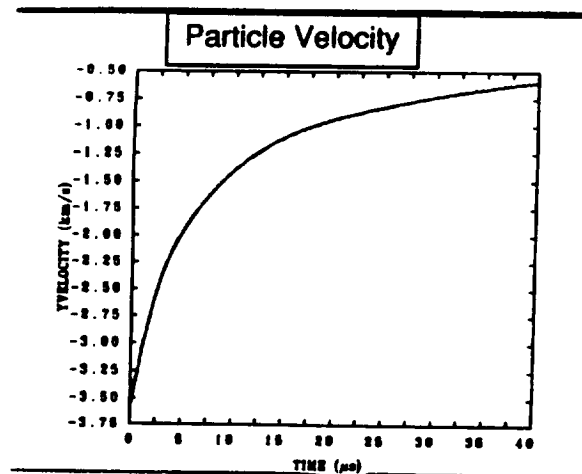


Figure 4.3-3: Kinetic Energy History.

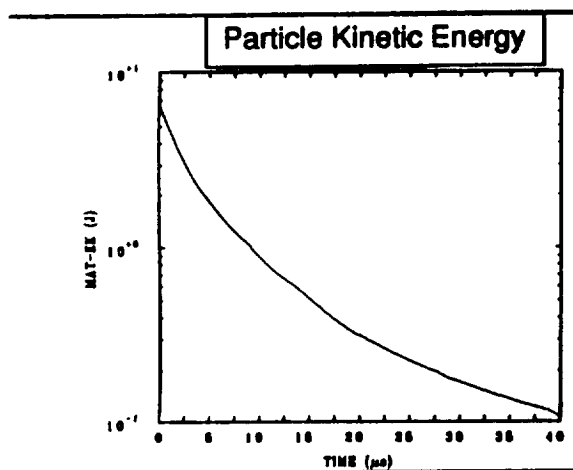


Figure 4.3-4: Particle Thermal Profile.

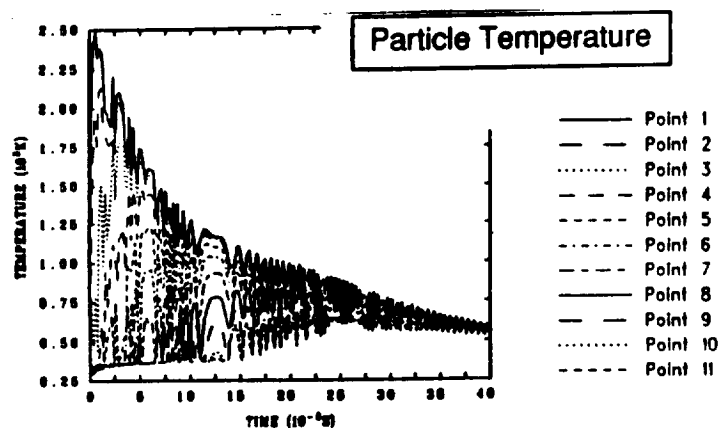
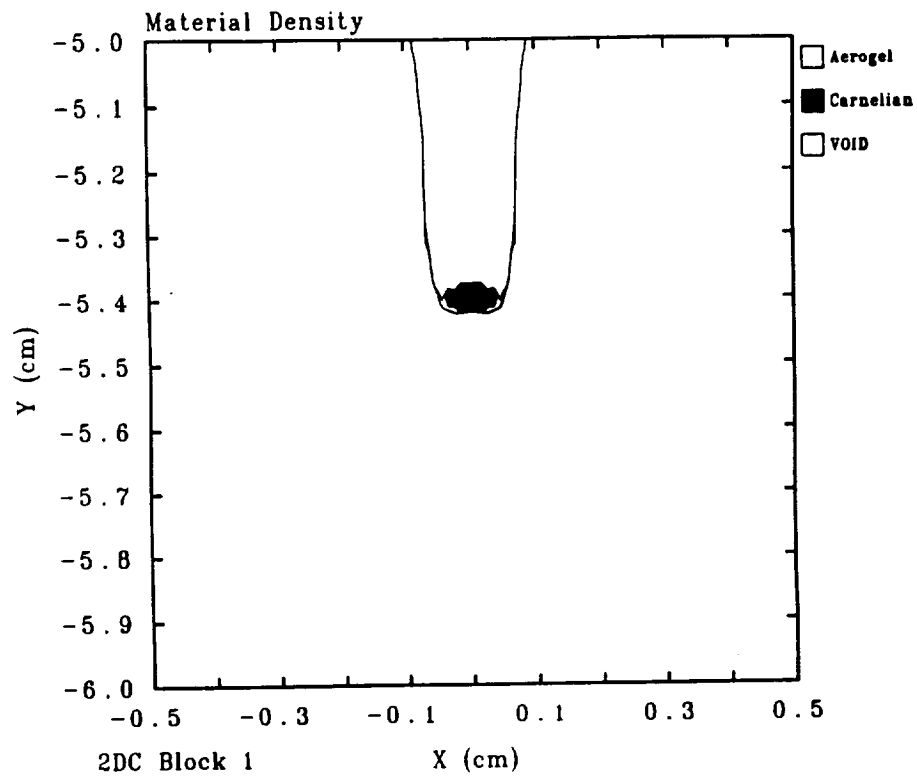
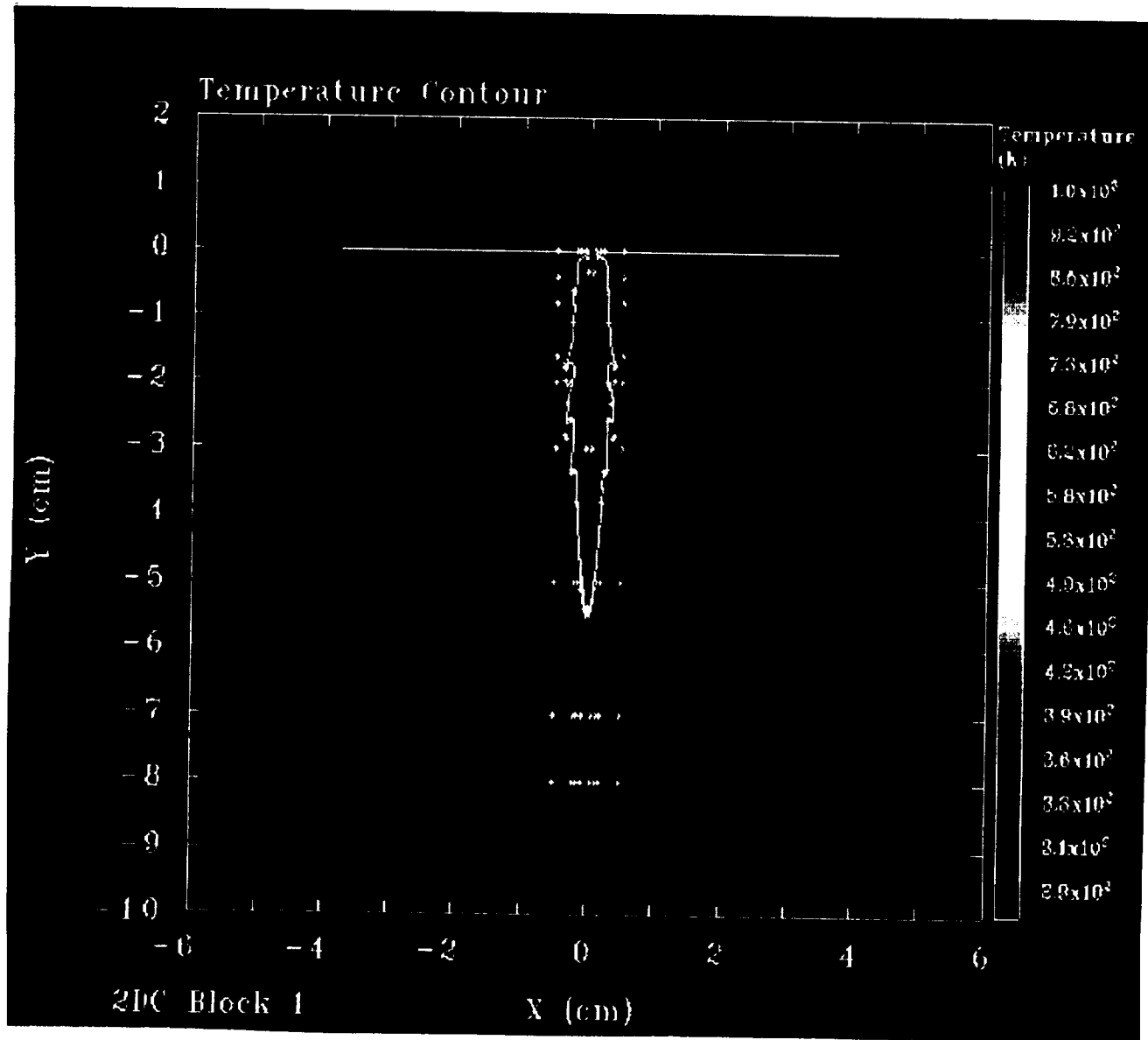


Figure 4.3-5 is an expanded view of the particle at 55  $\mu$  seconds. It shows that the particle maintained its diameter in the x-direction, but was compressed to half its original size in the y-direction. Physically this probably implies that the particle would fracture. Since the particle did not, in fact, fracture, this shows a shortcoming with this modeling approach. Figure 4.3-6 is the aerogel temperature contour of the model at the last time step.

#### 4.4 CONCLUSIONS

The CTH model approximated the aerogel track fairly well. Although the track depth was not achieved when the run terminated, enough kinetic energy remained in the particle that a deeper track depth can be expected if the run were allowed to proceed beyond 55  $\mu$  seconds. However, the model currently constrains the Carnelian particle to remain as a solid in order to better match the observed data with 3.58 km/sec particle velocity. Therefore, the model resulted in an unrealistic and physically impossible compression of the particle while requiring both an unrealistically high yield strength and spall stress. These assumptions and results imply shortcomings in this modeling approach. However, further changes could be made in the modeling assumptions which might eliminate some of these shortcomings. These changes were not explored due to funding constraints. The modeling results compared favorably enough with the experimental results that comparison with other approaches seems warranted.

**Figure 4.3-5: Expanded View of the Particle at 55  $\mu$  Seconds.**

**Figure 4.3-6: Aerogel Temperature Contour Plot at 55  $\mu$  Seconds.**

## SECTION 5.0

### APPLICATION TO PRACTICE: DESIGN, FABRICATION, AND LAUNCH OF AN AEROGEL FLIGHT MODULE

In the early phases of this program, techniques for preparation of high-purity aerogel suitable for IDP collection were demonstrated. In this phase of the program, these techniques were reduced to practice through the design, fabrication, and launch of an aerogel capture cell (ACC) for 1995 deployment on the European Science Exposure Facility (ESEF) aboard the Russian Mir Space Station. Provided below is a description of the ACC requirements, design, fabrication, pre-flight testing, and storage/shipping protocol. Also included, where appropriate, are lessons learned to be applied to future efforts in this area.

#### 5.1 AEROGEL CAPTURE CELL REQUIREMENTS

The ACC was fabricated for a joint NASA Ames/SETI/University of Paris experiment, conducted under the ESA-sponsored European Science Exposure Facility intended for deployment aboard the Russian Mir Space Station. This experiment was entitled COMRADE. For COMRADE, ACC requirements were provided by the European Space Agency (ESA) through the University of Paris, Institute of Space Astrophysics. These requirements included the following:

- Limitations on both dimensions and mass. COMRADE had a volume allowance for two ACC units, each having a footprint of 50.6 mm x 94.8 mm. The allowable height was 17 mm. These dimensions included attachment hardware. The target mass was 125 grams for each of the two ACC units.
- The instrument was required to meet outgassing restrictions so as not to contaminate either adjoining instruments or the IDP collection environment.
- The ACC was required to withstand temperature extremes experienced on orbit - specified as -125°C to +150°C.
- Detailed requirements were provided for tolerance to shock and vibration environments expected in all phases of shipment, delivery, launch, and recovery.
- The aerogel itself was required to meet functional requirements of an IDP capture medium: these included standards for purity, density, clarity, and homogeneity.
- Multiple ACC units were required for ground testing (2), archival storage (7), and actual flight (4). In all, 13 units were fabricated.

These requirements were integrated into an ACC design at the Palo Alto Research Center of Lockheed Missiles & Space Co., working in close collaboration with scientists and engineers from SETI, NASA Ames, and the University of Paris. The final design is detailed below.

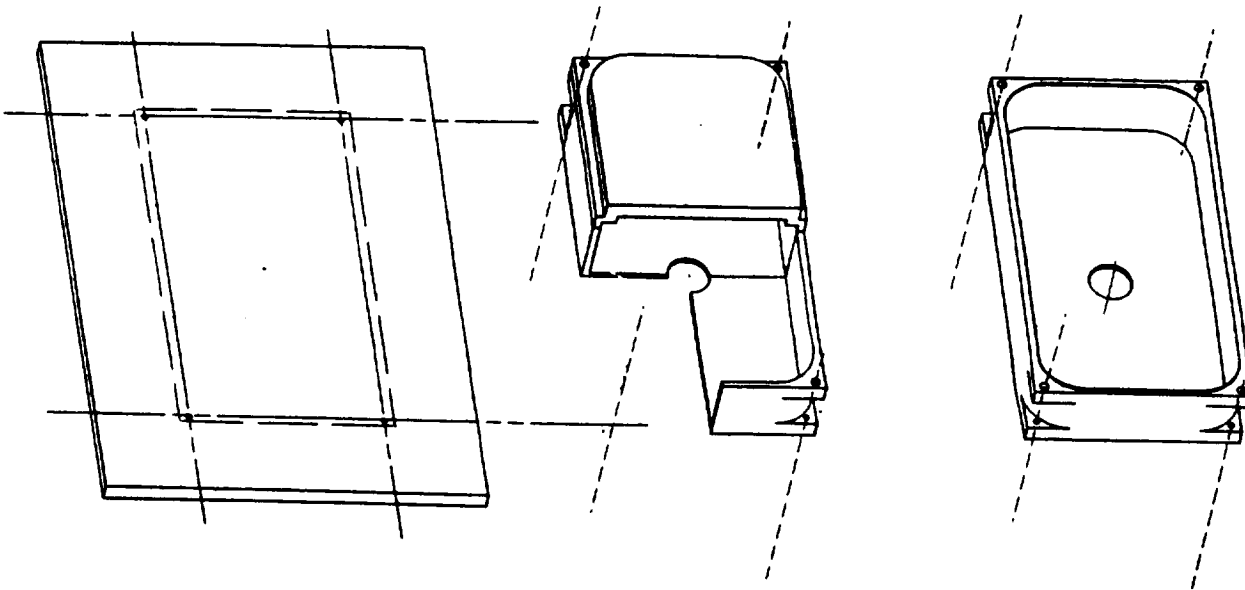
#### 5.2 AEROGEL CAPTURE CELL DESIGN

##### 5.2.1 Hardware Design

ACC hardware was designed to rigidly hold the aerogel, to be easily attached to the spacecraft, and to meet the weight and dimensional requirements. A schematic of an ACC is shown below in Figure 5.2.1.1. The overall envelope of this module is 50.6 mm x 94.8 mm. Attachment to the spacecraft is provided by steel screws placed at the corners of a 46 mm x 91 mm rectangle. The ACC container and lid were machined from 6061 aluminum alloy. The design weight of the container and lid was 90 grams.

The attachment screws were of austenitic stainless steel and had a size designation of M1.6 - corresponding to 1.5 mm diameter. The screws were designed to be tightened to a torque of 20 cN-m. Overall, the four screws for basal attachment and the four screws for lid attachment had a design weight of 4 g.

**FIGURE 5.2.1-1 Schematic of Aerogel Capture Cell showing mounting pad (left), ACC container and lid (center), and ACC container (right).**



### 5.2.2 Aerogel Specification

In keeping with the lessons learned in the Phase I effort of this program, the density of the aerogel was selected to be nominally 0.060 g/cm<sup>3</sup>. The aerogel was required to fit within a 47 mm x 92 mm x 15 mm envelope.

### 5.2.3 Assembly Methodology

The design for attaching the aerogel to the ACC aluminum container relied on the use of liquid metal encapsulation. This technique was chosen on the basis of lessons learned in the Phase I effort under this program. To meet the temperature requirements stated in 5.1, a low melting alloy composition of 55.5% Pb - 40.5% Sn - 4.0% Bi was selected. This alloy has a melting point of 198°C. Following liquid metal encapsulation, a wire grid system was designed to be placed over top of the aerogel tile and mechanically attached to the edge of the ACC aluminum container. The purpose of this grid is to retain aerogel chips that may tend to spall during an IDP impact event. The wire grid consisted of 0.075 mm diameter platinum wire.

## 5.3 AEROGEL CAPTURE CELL FABRICATION

### 5.3.1 ACC Hardware Fabrication

The ACC aluminum hardware was machined from aluminum alloy 6061 rolled plate. The as-machined weight of a typical ACC container was 34 g and the lid was 53 g.

To remove oils and other contaminants arising from the machining procedure, all aluminum ACC hardware was cleaned by hot degreasing, ultrasonic agitation in methylethylketone (MEK) for one hr, ultrasonic agitation in a fresh MEK bath for an additional 20 minutes, methanol rinse, and



drying in a nitrogen stream. All hardware was placed into polyethylene bags and sealed for storage.

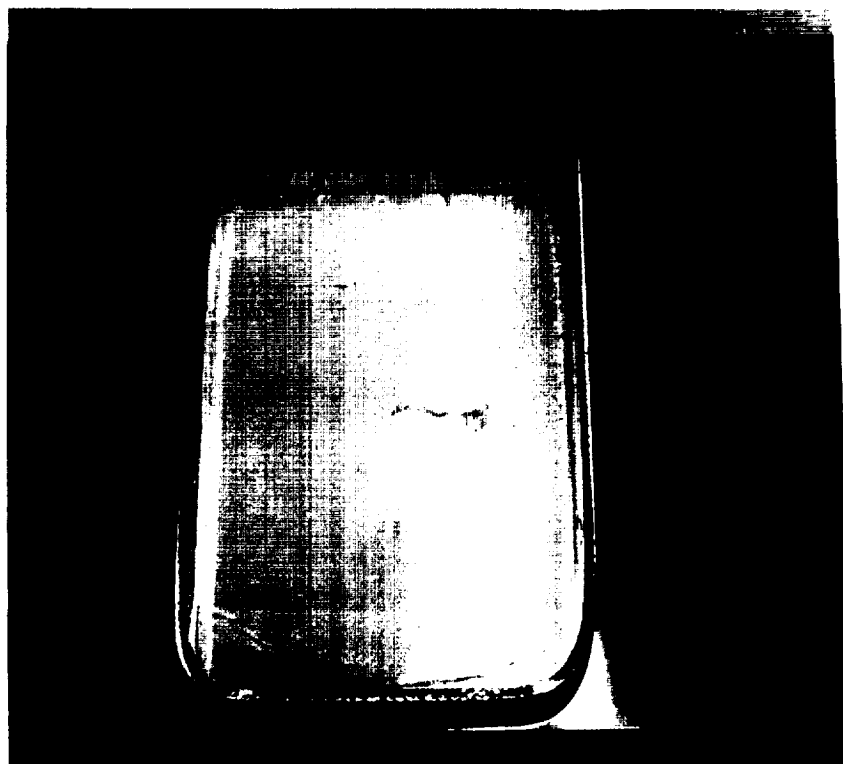
### 5.3.2 Aerogel Synthesis

Aerogel was synthesized at the Lockheed Palo Alto Aerogel Processing Facility. For this program, the base-catalyzed TMOS process with supercritical methanol extraction was employed. Chemical precursors formulated to yield a final density of  $0.060 \text{ g/cm}^3$  were cast into stainless steel molds having dimensions of 15 mm x 90 mm x 150 mm. The molds were constructed such that the "open end" of the mold was 15 mm x 90 mm. Prior to supercritical extraction, the alcogel was aged for ten days in a purified methanol bath. The supercritical extraction was performed using the following process parameters:

- Vessel pressure raised to 170 bars (17.2 MPa) over a 60 minute period using purified Argon gas.
- Vessel temperature raised to  $260^\circ\text{C}$  over a 5 hour period.
- Pressure was vented to achieve atmospheric pressure after 36 hr while slowly raising the temperature to  $330^\circ\text{C}$ .
- Vessel temperature lowered to room temperature over a 48 hr period while purging with purified Argon.

Following the extraction process, molds were disassembled and the aerogel tiles were carefully removed. Our method of mold construction resulted in "sawtooth" cracks along the edges of all tiles. However, the faces of all tiles were flat and defect-free. These aerogel tiles were trimmed to size using a band saw and fine emery papers. Handling at this stage included the use of white cloth gloves and the wearing of a respirator by our technician. These procedures were chosen so as to minimize contamination to the aerogel tiles during this "touch time" phase of processing. An example of the as-extracted aerogel tile and mold construction is shown in Figure 5.3.2.1.

**FIGURE 5.3.2-1 Aerogel tile with one face sheet removed from mold. Cracking observed at periphery but faces are defect free. The tile shown has dimensions of 150 mm x 90 mm x 15 mm.**



Following sizing, the aerogel tiles were wrapped as one lot of material into an aluminum foil container and subjected to a baking treatment in an oxygen environment. Included in this lot of aerogel were two "witness samples" for later chemical analysis. The aerogel was subjected to a 350°C bake for 36 hr. Following this baking procedure, a chemical analysis was performed. The results of this analysis are summarized in Table 5.3.2-1.

**Table 5.3.2-1 Chemical Analysis of Extracted and Baked Aerogel**

Sample Weight = 7.6 mg, MDL = 0.02 ppm

Cleaned 02/350C/36hr, semi-witness, 260C 15min flowing helium desorp. (3 times sequentially)

Impurity Concentration ppm (µg/g)	Impurity Concentration wt/wt %	Probable Compound
		CO2 artifact is the first eluting peak and is mostly due to room air CO2.
83.0	0.0083	methanol
12.0	0.0012	acetone
6.8	0.00068	methylethyl ketone (MEK)
0.1	0.00001	octamethyl cyclotetrasiloxane
0.6	0.00006	decamethyl cyclopentasiloxane
0.5	0.00005	n-C22.H46. hydrocarbon
3.0	0.0003	n-C23.H48. hydrocarbon
7.5	0.0007	n-C24.H50. hydrocarbon
10.0	0.0010	n-C25.H52. hydrocarbon
11.1	0.0011	n-C26.H54. hydrocarbon
8.5	0.0008	n-C27.H56. hydrocarbon
5.5	0.0005	n-C28.H58. hydrocarbon
2.9	0.0003	n-C29.H60. hydrocarbon
2.1	0.0002	n-C30.H62. hydrocarbon
0.4	1.00004	n-C31.H64. hydrocarbon
		other peaks are artifacts seen in blank run made just prior to sample run
Total 154	0.015	

The methanol and siloxane species observed are consistent with organic "impurities" seen in previously-processed aerogel - although the methanol level here is higher than desired at 83 ppm. The acetone and MEK impurities observed are a result of exposure of the aerogel to solvents during the post-extraction handling. This exposure was inadvertent and precautions will be instituted to prevent this in future efforts. The hydrocarbons observed have never been seen before as an impurity in LMSC aerogel, were not present in a companion witness coupon (see Table 5.3.3.1), and are assumed to be some type of rogue contaminant picked up during the chemical analysis procedure.

**Lessons Learned** The principal lessons learned at this stage were in the area of mold design:

- We found that aerogel tiles could not be made with adequate quality when the "open end" of the container corresponded to one of the tile faces, i.e. 90 mm x 150 mm. The best surface quality for the tile faces was ensured by using polished stainless steel face sheets in mold construction. In fact, our experience has resulted in the determination of a surface roughness specification that will be applied to mold construction materials in future programs.

- Further optimization of the mold design can still be achieved. We believe that the "sawtooth cracking" observed in our aerogel tiles is a result of sharp corners and surface irregularities inherent for our welded mold design. Molds which do not contain these discontinuities could yield net-shaped defect-free tiles. This would have the obvious advantage of producing tiles that would not require trimming to final shape.
- We learned that aluminum is not suitable as a mold material. Evidently, the supercritical extraction environment is highly corrosive to aluminum alloys and mold deterioration occurs readily.

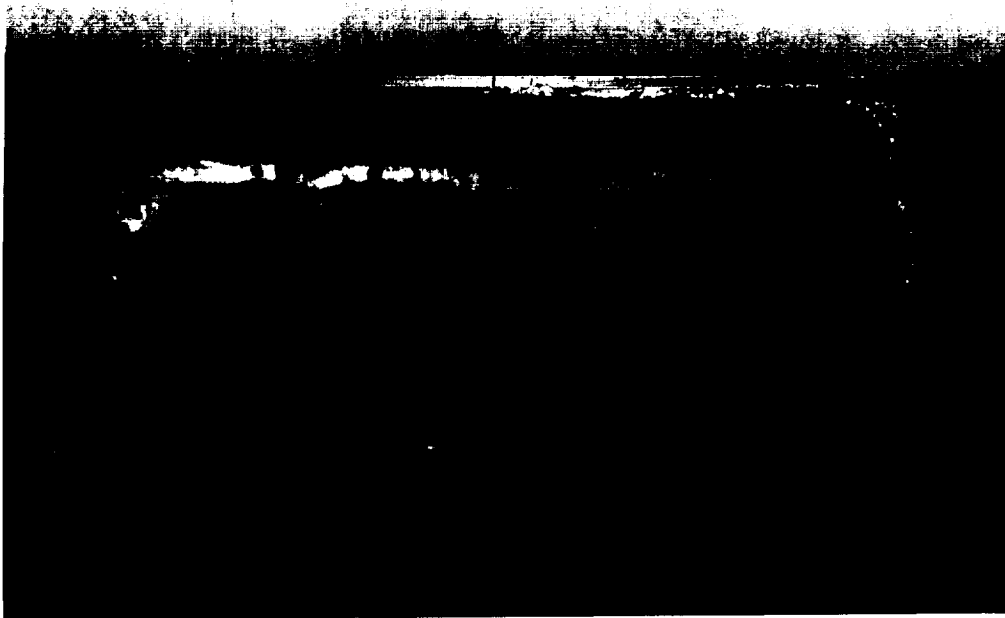
### 5.3.3 Bonding Procedures

The purpose of the bonding procedure was to cast a low-melting alloy around the aerogel in such a manner as to mechanically lock the aerogel into the ACC aluminum tray. As a precaution against aerogel loss during an IDP impact event, a grid of platinum wire was laid across the bonded aerogel tile and mechanically attached to edge of the aluminum tray. This completed assembly constitutes the aerogel capture cell.

The liquid metal encapsulation procedure was conducted under a fume hood to minimize exposure to toxic heavy metal fumes. Pre-weighed pieces of the low melting alloy were cleaned with MEK and acetone, placed into the ACC aluminum tray and heated to the melting point on an electric hot plate. An aerogel tile was then placed into the tray and the assembly was removed from the heat. This stage of processing is depicted below in Figure 5.3.3.1. A compressive force was applied to the surface of the aerogel to counter the buoyant forces associated with the liquid metal. This compressive loading was necessary to achieve liquid metal intrusion along the corners and edges of the aerogel tile, and hence, a high degree of bonding. The as-bonded ACC unit is shown below in Figure 5.3.3.2. The variations seen in the figure are actually in the low melting temperature alloy.

**FIGURE 5.3.3-1 Liquid metal encapsulation procedure.**



**FIGURE 5.3.3-2 As-bonded ACC unit**

Following the liquid metal encapsulation, a grid was constructed from fine platinum wires attached across the face of the aerogel capture cell. These wires were placed into machined slots and mechanically attached by pinching closed the slots with a hammer and punch set. This final assembly is shown in Figure 5.3.3.3, below.

The final stage of assembly consisted of attaching the lid to the aerogel capture cell, wrapping with Teflon tape for sealing, and placing the completed assembly into a polyethylene bag for storage.

Throughout this assembly operation, efforts were made to maintain the high cleanliness level of the aerogel. As a check of our overall effectiveness, a "witness coupon" accompanied one of the aerogel tiles through each phase of the ACC fabrication sequence. Following final assembly, this witness sample was subjected to GC/MS analysis for impurities. The results are as follows:

**Table 5.3.3-1: Chemical Analysis of Aerogel Witness Coupon**

Sample Weight =10.4 mg

Witness Sample, 260C 15min flowing helium desorp. (3 times sequentially)

Impurity Concentration ppm ( $\mu\text{g/g}$ )	Impurity Concentration wt/wt%	Probable Compound
		CO2 artifact is the first eluting peak and is mostly due to room air CO2.
58	0.0058	methanol
6.9	0.00069	acetone
4.9	0.00049	methylethyl ketone (MEK)
0.4	0.00004	octamethyl cyclotetrasiloxane
1.9	0.00019	decamethyl cyclopentasiloxane
		other peaks are artifacts seen in blank run made just prior to sample run
Total 72	0.0072	

This analysis shows that the residuals observed in the "as-baked" aerogel (Table 5.3.2.1) are also present at about the same level in the witness coupon. No other organic contaminants were accumulated as a result of ACC assembly.

**FIGURE 5.3.3-3 Final ACC assembly showing ACC unit (left) and lid (right).**



**Lessons Learned** The lessons learned at this stage were related to the apparent extreme reactivity of as-baked aerogel. This reactivity manifested itself in two ways:

- Initial attempts to counter the buoyancy forces associated with the liquid metal encapsulation utilized a glass platen. On the initial bonding trial, the glass platen became physically bonded to the aerogel tile. Initially, it was assumed that the silica aerogel was reacting with the silica glass to form a chemical bond. However, wrapping the glass platen with platinum foil did not alleviate the problem. Our final solution was to construct a platen from three quartz tubes. Using these tubes as rails, a compressive load could be applied to the aerogel with the minimum possible surface blemishing. The platen used and the resultant surface blemishes are shown below in Figure 5.3.3.4.
- The aerogel absorbed MEK and acetone that were stored in squeeze bottles in a far corner of the exhaust hood where the liquid metal encapsulation was taking place. This was the source of acetone and MEK residuals shown in Tables 5.3.2.1 and 5.3.3.1. Aerogel will not be exposed to organic solvents such as these in future efforts.

**FIGURE 5.3.3-4 Three-rail platen used to compressively load aerogel tile during the liquid metal encapsulation process. Note three longitudinal blemishes appearing on aerogel surface as a result of the loading.**

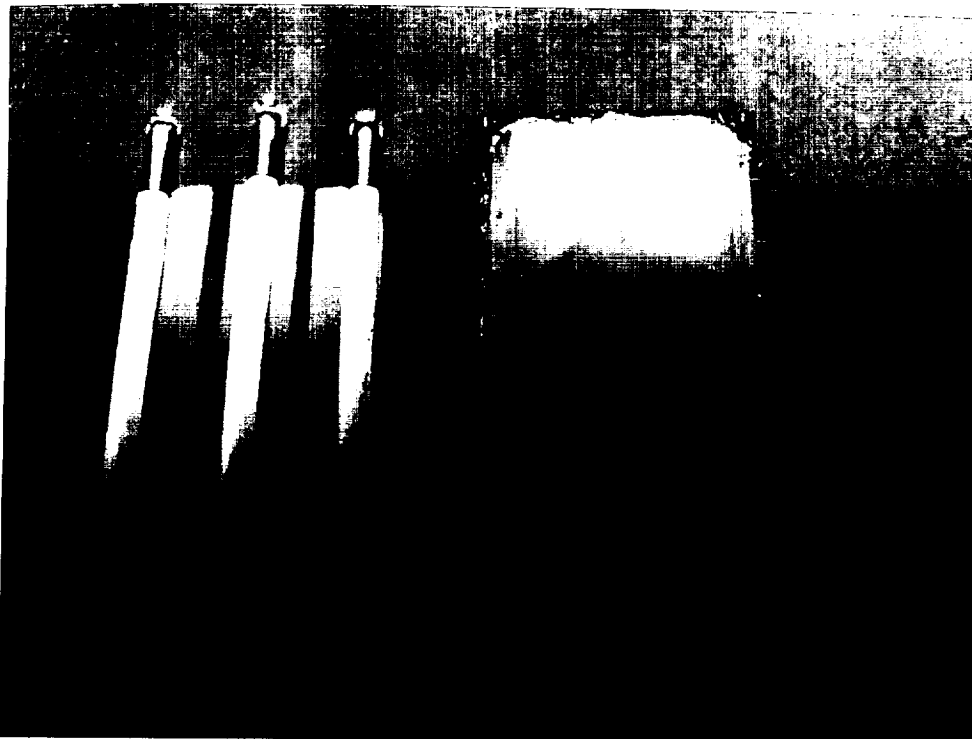


**FIGURE 5.3.3-5 Family of seven ACCs prior to packaging for shipment.**



## 5.4 AEROGEL CAPTURE CELL TESTING AND EVALUATION

### 5.4.1 Outgassing Analysis

The chemical analysis presented in Tables 5.3.2.1 and 5.3.3.1 adequately demonstrates that outgassing will be at a minimum for our ACC design. The chemical analysis presented above involves heating the aerogel to 200°C and collecting outgassing products in a helium stream for analysis. Based on our analyses, the aerogel can be expected to outgas ppm levels of acetone, methanol, and MEK while on orbit. Our method of attachment, based on use of a low-melting alloy, will not contribute to outgassing.

### 5.4.2 Shock and Vibration Analysis

Shock and vibration analyses representative of all phases of ground transportation, launch, deployment, re-entry, and recovery were conducted successfully. For all tests, "success" was defined as an ACC surviving the imposed loading spectrum without experiencing damage. Included in these tests were actual M1.6 screws planned for attachment of the ACC to the ESEF.

Shock and vibration testing was performed on a fully-assembled Aerogel Capture Cell. During the first (and most severe) test, a longitudinal crack developed in the aerogel tile. During all subsequent tests, this crack remained stable, did not increase in length or result in loss of aerogel material from the Aerogel Capture Cell. Other than this single incident, no other cracking was noted during the shock and vibration tests. The tests performed and results obtained are summarized as follows:

**TABLE 5.4.2-1: Shock and Vibration Testing†**

Test Description	Test Parameters	Test Results
Return in Soyuz (per ESA Requirement 4.1.3)	Random Vibration: 3500 seconds, X, Y, Z axes	Small Longitudinal Planar Crack Develops
Ground Transportation (per ESA Requirement 4.2.1)	Shock Testing 9g, X, Y, Z axes	Passed
Launch in Progress (per ESA Requirement 4.2.2)	Shock Testing 40g, X, Y, Z axes	Passed
Return in Soyuz (per ESA Requirement 4.2.3)	Shock Testing 50-100g, X, Y, Z axes	Passed
Linear Acceleration (per ESA Requirement 4.3.2)	Centrifuge 2-6g, X, Y, Z axes, 600 sec	Passed
Linear Acceleration (per ESA Requirement 4.3.3)	Centrifuge 7.3g, X axis	Passed

† All Requirements per ESA-ESEF-201, 28 Nov. 1994

Following shock and vibration testing, this ACC unit was retained for archival purposes.

Successful completion of these tests constitutes a major milestone for our aerogel program. These data show that our unique ACC design is fully capable of meeting the most stringent of shock and vibration loadings.

## 5.5 PROCEDURES FOR SHIPMENT AND STORAGE

To ensure practical and safe handling of the ACC units during shipping, mounting, deployment, and recovery, instructions were prepared and sent to the University of Paris team in advance of the aerogel shipment. These instructions are duplicated below.

### Un-Packaging

- 1 Aerogel is Packaged in a wooden packing crate. This crate contains
  - (1) Cylindrical Canister with four (4) Aerogel Capture Cells (Note: Lid of shipping canister contains a porous metal plug to equalize ambient and internal pressures during shipping.)
  - (1) Torque Wrench with 1.5 mm Driver
  - (1) 2.0 mm Hex Wrench
  - (2) Pilot Hole Drill Bits for BASAL SCREWS
  - (2) 1.5 mm taps for BASAL SCREWS
  - (1) Tap Handle
- 2 Remove Lid from Cylindrical Canister by first removing sealing tape from circumference.
- 3 Within the canister are four (4) aerogel capture cells, a set of eight (8) 1.5 mm x 7 mm BASAL SCREWS, an extra set of 10 (10) 1.5 mm x 8 mm screws, and foam rubber packaging material. Carefully remove the four aerogel capture cells and the screws.

### Mounting Aerogel Capture Cells

- 1 Remove protective wrap from periphery of Aerogel Capture Cells. Note that two cells are denoted with an "A" on the lids and 2 are denoted with a "B". Although all units are usable, we feel that the overall manufacturing quality of the "A" units is superior. We suggest that the "A" units be used as the primary flight hardware.
- 2 Refer to attached drawing (Figure 5.5.1) and note that locations of the 2.0 mm screws which secure the lid in place (LID SCREWS) are denoted as A, B, C, and D. The locations of the 1.5 mm screws which secure the aerogel capture cell in place (BASAL SCREWS) are denoted as A', B', C', and D'.
- 3 Loosely place all BASAL SCREWS in holes at locations A', B', C', and D'.
- 4 Using the 2.0 mm Hex Wrench, remove LID SCREWS located at A and C.
- 5 Using the 1.5 mm Hex attachment for the torque wrench, insert the BASAL SCREWS at locations A' and C'. Tighten screws to a torque value of 20 cN-m.
- 6 Replace LID SCREWS to locations A and C.
- 7 Repeat steps 4-6 with respect to locations B and D, B' and D'.
- 8 Lid is to remain in-place on Aerogel Capture Cell until latest possible moment prior to launch.

### Dismounting Aerogel Capture Cells

- 1 Place LID over Aerogel Capture Cell as soon as cassette is opened.
- 2 Remove the BASAL SCREWS in the reverse order as mounting.
- 3 Place sealing tape around the periphery of the Aerogel Capture Cells
- 4 Repack in cylindrical canister and into wooden shipping container.
- 5 Include Torque Wrench, 1.5 mm Driver, and 2.0 mm Hex Wrench, drills, taps, and tap handle in wooden crate.



These procedures are expected to result in a minimum of contamination during shipping, mounting, deployment, and recovery.

## **5.6 SUMMARY**

The preparation of the ACC flight modules described above constituted a major milestone in our efforts at LMSC to develop aerogel technology suitable for NASA applications. Firsts for our program include preparation of defect-free pre-specified aerogel geometries, validation of our aerogel attachment scheme, and successful completion of shock and vibration testing. Most importantly, the lessons learned and experience gained position us to approach future efforts with added confidence, cost realism, and schedule realism.

